# Dispersing quasinormal modes in (2+1)-dimensional conformal field theories

William Witczak-Krempa and Subir Sachdev

Phys. Rev. B **87**, 155149 — Published 29 April 2013

DOI: 10.1103/PhysRevB.87.155149

# Dispersing quasinormal modes in 2+1 dimensional conformal field theories

William Witczak-Krempa
*Perimeter Institute for Theoretical Physics, Waterloo, Ontario N2L 2Y5, Canada*

Subir Sachdev
*Department of Physics, Harvard University, Cambridge, Massachusetts, 02138, USA*

(Dated: April 10, 2013)

We study the charge response of conformal field theories (CFTs) at non-zero temperature in 2+1 dimensions using the AdS/CFT correspondence. A central role is played by the quasinormal modes (QNMs), specifically, the poles and zeros of the current correlators. We generalize our recent study of the QNMs of the a.c. charge conductivity to include momentum dependence. This sheds light on the various excitations in the CFT. We begin by discussing the R-current correlators of the $\mathcal{N} = 8$ SU($N_c$) super-Yang-Mills theory at its conformal fixed point using holography. For instance, transitions in the QNM spectrum as a function of momentum clearly identify "hydrodynamic-to-relativistic" crossovers. We then extend our study to include four-derivative terms in the gravitational description allowing us to study more generic charge response as well as the role of S-duality, which plays a central role in understanding the correlators. The presence of special purely-damped QNMs can lead to new behavior, distinct from what occurs in the aforementioned gauge theory. We also extend previous conductivity sum rules to finite momentum and discuss their interpretation in the gravity picture. A comparison is finally made with the conformal fixed point of the vector O($N$) model in the large-$N$ limit.

## I. INTRODUCTION

The subject of strongly-coupled quantum criticality (QC) without well-defined quasiparticle excitations has long been an important focus of the study of correlated electron systems. The simplest examples of such states in two spatial dimensions are provided by quantum critical points described by conformal field theories (CFT3s). The traditional condensed matter approach to the non-zero temperature dynamics of such systems has been to apply the quantum Boltzmann equation, and related perturbative field-theoretic methods[1]. However, such methods are designed for systems with long-lived quasiparticles, and the range of their applicability to systems without quasiparticles is unclear. The AdS/CFT correspondence[2] has provided a new set of tools to investigate the dynamics of QC[3]: an important advantage of this method is that quasiparticles do not appear at any stage in the computation, and even the leading results do not contain artifacts linked to the existence of long-lived quasiparticles. Instead, a simple picture of the dynamics emerges in terms of the *quasinormal modes* (QNMs) of a gravitational theory on an asymptotically Anti de Sitter (AdS) spacetime. In a recent paper we described the structure of these QNMs in some detail for spatially uniform probes[4]. This paper will extend the analysis to allow for spatial dependence, and describe the dispersion of the QNMs as a function of spatial momentum. As we shall see, this yields far deeper insights than the zero-momentum response.

Our objects of study are two-point correlation functions of currents in thermally excited CFT3s. Expressed in frequency-momentum space these are $\langle J_\mu(\omega,\boldsymbol{k})J_\nu(-\omega,-\boldsymbol{k})\rangle$, where the average is over the thermal density matrix, while $\mu,\nu$ are spacetime indices. Such correlators yield, for instance, the frequency-dependent charge conductivity in the limit of vanishing momentum. We emphasize that such current correlators can be probed experimentally in QC systems with emergent Lorentz invariance. An important example is the quantum phase transition between a bosonic Mott insulator and a superfluid in two spatial dimensions, which is described by the well-known QC O(2) model. Recent experiments with ultra-cold atoms in optical lattices have realized such a QC point, both in three[5] and two[6–8] dimensions. The excellent control in these experiments gives hope that the universal QC charge response could be measured in the near future. On the other hand, as interactions are strongly relevant in such critical systems, the theoretical description of many quantities remains very challenging, especially concerning the current correlators of the U(1) charge in real time and at finite temperature. Holographic methods have successfully yielded some fresh insights into the problem at hand[3,4,9,10]. For instance, the frequency-dependent conductivity of a strongly correlated CFT (with supersymmetry) has been exactly computed[3] using the AdS/CFT correspondence[2]. It was remarkably found that the conductivity does not vary with frequency because of an emergent self-duality, which is not expected to hold for generic CFTs. Further extensions[9,10] of the original holographic model have yielded frequency-dependent conductivities that can be expected in quantum fluids with particle- or vortex-like excitations. A sharp distinction between the two types of response can be made by examining the correlators at complex frequencies[4]: the particle-like conductivity has a pole at a frequency of order $-iT$, whereas the vortex-like conductivity has a *zero* there. These become manifest at real frequencies by the presence of a maximum or minimum at zero frequency, respectively. In the former case, a small-frequency peak is obtained to which we refer as the Damle-Sachdev (DS) peak[11]. At a formal level, it shares the same single-pole structure as the Drude peak characterizing the transport of a gas of electrons subject to a source of inelastic scattering (disorder). An important difference is that translation symmetry is not broken in a CFT, instead the finite d.c. conductivity results from the particle-hole symmetry at zero charge density. This is why we choose the designation DS instead of "Drude".[12]

The poles and zeros of the retarded correlators, the QNMs, acquire a significant physical meaning for the correlated CFT: they are excitation modes of the system. In this sense, understanding how they propagate or disperse as a function of momentum yields important insight into the excitation channels of the CFT. In a certain sense, the QNMs supersede the concept of weakly interacting quasiparticles. Interestingly, the AdS/CFT correspondence connects these QNMs with discrete excitation modes of a black hole in one higher dimension[13–15], which allows for the inclusion of a finite temperature. In the case of the QNMs of the current correlators, these excitations correspond to electromagnetic "eigenmodes" of the black hole. The holographic correspondence thus identifies the "normal" modes of black holes with the emergent excitations of a strongly correlated CFT[13–15]. We mention that such QNMs have been explored

in a variety of different holographic applications to strongly correlated systems potentially relevant to condensed matter[3,4,16–20]. A recent review by Hartnoll[21] covers a number of these, with special focus on the QNMs.

### A. Main results

The CFT current correlators are obtained holographically via a general four-derivative bulk action[9,10], which in one limit describes the R-current correlators of an $\mathcal{N} = 8$ superconformal gauge theory[3]. The correlators are found to bear a strong imprint from their $T = 0$ Lorentz invariant form, such as a "reflection" property between the real and imaginary parts under exchange of frequency and momentum, illustrated in Fig. 1. In almost the entire frequency-momentum domain, except in the hydrodynamic regime, the correlators can indeed be interpreted as "smoothed" versions of the relativistic forms. The "smoothing" occurs via the breakup at finite temperature of the $T = 0$ branch cuts into a discrete sequence of poles and zeros, the QNMs. We further identify sharp transitions in the QNM spectrum as a function of momentum, and these manifest themselves at real frequencies as hydrodynamic-to-relativistic crossovers. In this respect, we emphasize how the presence of a four-derivative term in the bulk action can lead to distinct behavior compared to the leading two-derivative Einstein-Maxwell action. The latter is self-dual under an electric-magnetic duality[3], and this constrains the correlators considerably. Higher order terms will break this self-duality[10], and in particular give rise to a special QNM on the imaginary frequency axis, referred to as the D-QNM due to its purely damped nature and its formal relation to the usual Drude scaling. This QNM lies at the heart of the difference between the particle- and vortex-like responses and it is expected to be present in generic CFT3s[4,22], and indeed appears in the four-derivative holographic theory. As we have noted above, when this D-QNM is a pole, it gives rise to a small-frequency DS peak in the conductivity, whereas a valley results when it is a zero.

A generalization of particle-vortex duality, S-duality[23], which manifests itself as electric-magnetic duality in the bulk, plays a central role in our analysis. It leads for instance to the appearance of a hydrodynamic zero in the transverse response (i.e. when the current is transverse to the momentum). This zero becomes the standard hydrodynamic pole $\omega \sim -i\hat{D}k^2$ of the S-dual theory, where $\hat{D}$ is the S-dual diffusion constant. S-duality is also central in the sum rule analysis, which we extend to finite momentum, see Eq. (38) and Eq. (41). The conductivity sum rules[4,20] obtained at zero momentum, for both the direct and S-dual[4] theories, are found to rely on the bulk gauge invariance of the gauge field holographically dual to the CFT current operator. We finally conclude with a comparison with the vector O($N$) model at its large-$N$ conformal fixed point. For instance, we find an analogous sum rule to what is obtained in the holographic analysis, including an almost exact agreement between static correlators entering the sum rules.

The outline is as follows: We first discuss general properties of current correlators in CFT3s in Section II. We then turn to their explicit study in a supersymmetric gauge theory using the AdS/CFT correspondence in Section III. We extend the analysis to more generic holographic models including a four-derivative bulk term in Section IV. Sum rules are discussed in Section V, and finally a comparison with the vector O($N$) model is made in Section VI, followed by a conclusion.

## II. CURRENT CORRELATORS IN A CFT

We first review some general properties of the current correlators in CFT3s, namely the meromorphic structure in Subsection II A and the asymptotics in Subsection II B.

### A. Physical imprint in the analytic structure

In the holographic models we consider below, the finite-temperature current correlators will be meromorphic in the complex frequency plane, i.e. they will be analytic except at a discrete set of finite order poles. Moreover all the poles (and zeros) will be in the lower half-plane (LHP) of frequency by virtue of retardedness. One can ask: To what extent are these properties generic? For instance, it is well-known that the zero-momentum correlators,

which give the conductivity, will generically have a branch cut at frequencies whose norm is much less than the temperature. This branch cut emanates from the zero frequency point and is associated with the so-called long-time tails of hydrodynamics[24,25], following from the presence of gapless hydrodynamic modes at arbitrary long-wavelengths, such as the well-known diffusive mode discussed below. At finite momentum, however, the length scale introduced in the problem is expected to introduce an IR cutoff beyond which correlators decay exponentially and not algebraically, thus excluding branch cuts of that sort. Such arguments seem reasonable as they are based on the universal principles of hydrodynamics. But what about frequencies whose norm is of the order or greater than the temperature and thus fall beyond the hydrodynamic regime? In that case, a statement regarding general interacting CFTs is hard to establish, but it is not unreasonable to expect that a slightly (read infinitesimally) perturbed thermal CFT state will relax back to *local* equilibrium exponentially fast, which is tantamount to assuming that no branch cuts will emanate from the real axis. This does not preclude the presence of branch cuts in the LHP away from the real frequency-axis. These are absent in the holographic models we study, but it is at present unclear if CFT3s will generically obey this rule. It would be interesting to investigate this aspect in more detail by considering specific CFTs, such as the O($N$) vector model at finite but large $N$. (The $N \to \infty$ is discussed in Section VI.)

To gain further insight into the role of the QNMs, let us consider a generic meromorphic current correlator, as obtained using holography for instance:

$$\begin{aligned}\langle J_\mu(\omega,\boldsymbol{k})J_\nu(-\omega,-\boldsymbol{k})\rangle &= a\frac{\prod_m(\omega-\hat{\omega}_k^m)}{\prod_n(\omega-\omega_k^n)}\\ &\to \sum_n a_n \exp\left(-|\Im\omega_k^n|t - i\Re\omega_k^n t\right)\,, \end{aligned} \tag{1}$$

where $a$ is a constant and the arrow indicates a temporal Fourier transform. Note that we are leaving out the delta function $\langle J_\mu(k_\alpha)J_\nu(k'_\alpha)\rangle = \delta^{(3)}(k_\alpha + k'_\alpha)C_{\mu\nu}(k_\alpha)$. Each pole QNM, $\omega_k^n$, contributes an exponential to the time-dependence of the correlation function. As all the poles are in the LHP, the exponentials decay in time. We thus see that the QNMs closest to the real axis will dominate the long-time response of the system since they correspond to the longest decay time-scales. On the other hand, the real part of the QNM frequency provides the oscillatory behavior. As the momentum $k$ increases from zero to infinity, these time scales will change and lead to very different behavior. In the language of the excitation modes of the system, the absolute value of the imaginary part gives the lifetime of the excitation, while the real part its energy. A so-called quasiparticle mode will have an energy much greater than its lifetime; while purely damped modes do not have a real part, such as the diffusion pole. The momentum dependence of these modes gives generalized dispersion relations for the excitations. In the case of the quasiparticle QNMs, this replaces the usual energy-momentum dispersion relation of weakly interacting quasiparticles.

The zeros, $\hat{\omega}_k^n$, play an important role as well. Not only are they essential to determine the values of the correlator, but in the theories we consider below, they also correspond to the QNM excitations of the S-dual theory. S-duality (see 23 for its action on CFT3s) is a generalization of the usual particle-vortex duality familiar in the context of the O(2) model describing the superfluid-to-insulator quantum phase transition.

Finally, as we argue below, the QNMs evolve into branch cuts in the limit of zero temperature where one recovers power law decay in time of the correlation functions, in accordance with the behavior expected to take place directly at the fixed point. This is physically clear given that the QNM excitations merge and form a continuum.

### B. Symmetries and asymptotic forms

We now review the symmetries and asymptotic behavior of the current correlators. This will serve as an important comparison point throughout the work. Although most of the discussion follows Ref. 3, we make new remarks regarding the hydrodynamic behavior of the transverse current correlators, which naturally leads to S-duality. We consider correlation functions involving two conserved currents, $J_\mu^a(x)$, in a CFT at finite temperature, where $\mu$ is the spacetime index, while $a$ labels the flavor. The Fourier transform of the retarded current correlator, $C_{\mu\nu}^{ab}(x) =$

$-i\theta(x^0)\langle[J^a_\mu(x), J_\nu(0)]\rangle$, can be decomposed as follows

$$C^{ab}_{\mu\nu}(\omega, \boldsymbol{k}) = P^L_{\mu\nu}\Pi^L_{ab}(\omega, k) + P^T_{\mu\nu}\Pi^T_{ab}(\omega, k)\,, \tag{2}$$

where two sets of functions, $\Pi^L_{ab}$ and $\Pi^T_{ab}$, are needed because the temperature breaks the Lorentz invariance. Note that $C^{ab}_{\mu\nu}/T$ depends only on the rescaled frequency $\omega/T$ and momentum $\boldsymbol{k}/T$, the latter ratio arising since a CFT has a dynamical exponent $z = 1$. We work in units where $c = \hbar = k_B = 1$ throughout. The transverse projector reads

$$P^T_{tt} = P^T_{ti} = P^T_{it} = 0, \quad P^T_{ij} = \delta_{ij} - \frac{k_i k_j}{\boldsymbol{k}\cdot\boldsymbol{k}}\,, \tag{3}$$

and by orthogonality: $P^L_{\mu\nu} = [\eta_{\mu\nu} - k_\mu k_\nu/k\cdot k] - P^T_{\mu\nu}$, where $k^\mu = (\omega, \boldsymbol{k})$ and roman indices run over spatial coordinates. The Minkowski metric was introduced, $\eta_{\mu\nu} = \mathrm{diag}(-1, 1, 1)$, such that $k\cdot k = \eta_{\lambda\lambda'}k^\lambda k^{\lambda'} = -\omega^2 + k^2$. It is easy to see that $C^{ab}_{\mu\nu}(\omega, \boldsymbol{k})$ is symmetric in $\mu, \nu$ and satisfies the Ward identity $k^\mu C^{ab}_{\mu\nu}(\omega, \boldsymbol{k}) = 0$ resulting from current conservation. Both of these properties are in fact independently satisfied by the projectors, $P^{L,T}_{\mu\nu}$.

Due to the rotational invariance, we are free to fix the momentum to point along the $x$-direction, $\boldsymbol{k} = (k, 0)$, which yields

$$C^{ab}_{tt}(\omega, \boldsymbol{k}) = \frac{k^2}{\omega^2 - k^2}\Pi^L_{ab}\,; \quad C^{ab}_{xx}(\omega, \boldsymbol{k}) = \frac{\omega^2}{\omega^2 - k^2}\Pi^L_{ab}\,, \tag{4}$$

$$C^{ab}_{yy}(\omega, \boldsymbol{k}) = \Pi^T_{ab}\,. \tag{5}$$

Also, $C^{ab}_{tx} = C^{ab}_{xt} = -\frac{\omega k}{\omega^2 - k^2}\Pi^L$ while all the ones mixing $y$ with $x$ or $t$ vanish, in line with the decoupling between longitudinal and transverse responses. In the limit of zero temperature, a simple form dictated by Lorentz invariance emerges:

$$C^{ab}_{\mu\nu}(\omega, \boldsymbol{k})\big|_{T=0} = \left(\eta_{\mu\nu} - \frac{k_\mu k_\nu}{k\cdot k}\right)\sqrt{k\cdot k}K_{ab}\,, \tag{6}$$

where $K_{ab}$ are the conductivities in the $\omega/T \to \infty$ limit: $K_{ab} = \sigma^{ab}_\infty$. We choose the branch of the square root $\sqrt{k\cdot k}$ to be in the LHP $\omega$-plane and such that $\Im\sqrt{k\cdot k} > 0$ when $w > q$. Specifically, the charge and transverse current correlators read:

$$C^{ab}_{tt}(\omega, \boldsymbol{k})\big|_{T=0} = \frac{k^2}{\sqrt{-\omega^2 + k^2}}K_{ab}\,, \tag{7}$$

$$C^{ab}_{yy}(\omega, \boldsymbol{k})\big|_{T=0} = -\sqrt{-\omega^2 + k^2}K_{ab}\,. \tag{8}$$

We note that these functions have branch points at $\omega = \pm k$: $C_{tt}$ has branch poles while $C_{yy}$ branch zeros.

At finite temperature and in the opposite limit of small frequency and momentum, $|\omega|, k \ll T$, we obtain hydrodynamic behavior. For example, the correlators of the conserved charge densities, $J^a_t$, read

$$C^{ab}_{tt}(\omega, k) \approx \sum_\ell \frac{\chi^\ell_{ab}D_\ell k^2}{i\omega - D_\ell k^2}\,, \quad |\omega|, k \ll T\,, \tag{9}$$

where $\ell$ sums over the diffusive eigenmodes; $\chi^\ell_{ab}$, $D_\ell$ are the corresponding charge susceptibilities and diffusion constants, respectively. By virtue of scaling: $\chi_{ab} = T\bar{\chi}^\ell_{ab}$ and $D_\ell = \bar{D}_\ell/T$, with $\bar{\chi}^\ell_{ab}, \bar{D}_\ell$ being universal dimensionless quantities associated with the conformal fixed point, just like the $K_{ab}$ introduced in Eq. (6). They are related to the d.c. conductivities via Einstein relations: $\sigma^{ab}_{\mathrm{dc}} = \sum_\ell \chi^\ell_{ab}D_\ell$. Crucially, the hydrodynamic charge response is characterized by the presence of diffusive poles in the LHP $\omega$-plane at $\omega = -iD_\ell k^2$. In the same limit, we propose that the

transverse current correlator is given by

$$C^{ab}_{yy}(\omega,k) \approx -\sum_{\ell} \chi^{\ell}_{ab} D_\ell (i\omega - \tilde{D}_\ell k^2)\,, \tag{10}$$

where the tilde variables $\tilde{D}_\ell$ obey the same scaling as their cousins $D_\ell$. We shall see that in theories for which we can define S-duality, these are the diffusion constants of the S-dual theory. Contrary to $C_{tt}$, the hydrodynamic behavior of the transverse correlator is analytic. However, it has analogs to the diffusive poles: a set of "diffusive zeros" at $\omega = -i\tilde{D}_\ell k^2$. When S-duality exists, it will map these to the diffusive poles of the S-dual theory.

## III. $\mathcal{N} = 8$ SUPER-YANG-MILLS

We first examine a special theory whose holographic description is believed to be very simple: it is a 2+1D Yang-Mills theory with gauge group SU($N_c$) and $\mathcal{N} = 8$ supersymmetry[26]. In a certain large-$N_c$ limit, the theory flows to a strongly coupled CFT. Further, it is believed that this CFT admits a holographic description in terms of a string theory (or rather its 10+1D extension, M-theory). The holographic duality maps the vacuum of the CFT to a stack of $N_c$ M2-branes which can be described by M-theory on $\mathrm{AdS}_4 \times S_7$. In the large-$N_c$ limit, the M-theory reduces to classical supergravity and the AdS/CFT correspondence allows one to relate the correlators of the classical gravity on $\mathrm{AdS}_4$ to those of the CFT living in one lesser spatial dimension. In particular, the CFT has a set of SO(8) R-symmetries, which map to the symmetries of the sphere $S_7$ via the holographic correspondence. The R-symmetries can be thought of as rotations amongst the $\mathcal{N} = 8$ supercharges, which get mapped to rotations of the 7-sphere in the dual theory.

The correlators of the $28 = \binom{8}{2}$ R-currents $\{J^{a=1,\ldots,28}_\mu\}$ are entirely encoded in two functions, $\Pi^{L,T}$, due to the SO(8) symmetry:

$$C^{ab}_{\mu\nu}(\omega,\boldsymbol{k}) = \delta_{ab}\left[P^L_{\mu\nu}\Pi^L(\omega,k) + P^T_{\mu\nu}\Pi^T(\omega,k)\right]\,. \tag{11}$$

Only the diagonal correlators remain finite allowing us to drop the flavor indices. A further simplification was shown to exist[3] because of the presence of a self-duality which manifests itself as an electric-magnetic duality in the gravitational description. As a result, the longitudinal and transverse correlators are directly related:

$$\Pi^L(w,q)\Pi^T(w,q) = \chi_0^2(-w^2+q^2)\,, \tag{12}$$

where we have introduced the rescaled frequency and momentum:

$$w = \frac{3\omega}{4\pi T}\,, \qquad q = \frac{3k}{4\pi T}\,. \tag{13}$$

We have also introduced the charge susceptibility[3] $\chi_0 = (4\pi T/3)g_4^{-2}$, where $g_4^{-2} = (\sqrt{2}/6\pi)N_c^{3/2}$ is the inverse coupling squared of the gauge field holographically dual to a given R-current, as discussed in more detail below. It should be noted that that the frequency and momentum are rescaled by the diffusion constant, $D_0 = 3/4\pi T$, which is related to $\chi_0$ by the Einstein relation $D_0\chi_0 = \sigma_0$, where the d.c. R-charge conductivity is $\sigma_0 = 1/g_4^2$. By virtue of the self-duality mentioned above, the a.c. conductivity was remarkably found to be frequency independent[3], a fact to which we return in the next section.

We finally note that as a result of Eq. (12), the charge correlator $C_{tt}$, Eq. (4), can be expressed in terms of the transverse one, $\Pi^T = C_{yy}$:

$$C_{tt}(w,q) = -\frac{\chi_0^2 q^2}{\Pi^T(w,q)} \tag{14}$$

### A. Bulk action for boundary correlators

We introduce the basic holographic tools needed to compute the correlators and refer the reader to some reviews aimed at condensed matter researchers for further background on this rich topic[21,27–29]. In the AdS/CFT correspondence, the global currents in the CFT are dual to gauge fields in the bulk. Since the current correlators are diagonal in the R-charge flavor index, and the bulk gauge coupling tends to zero in the large-$N_c$ limit we can focus on a single $U(1)$ gauge field $A_a(t,x,y,r)$ instead of considering the full non-abelian SO(8) gauge structure. The coordinate $r$ is along the extra spatial dimension. This gauge field will be dual to a current operator $J_\mu(t,x,y)$ that can be thought to live on the boundary at $r=\infty$. The AdS/CFT correspondence relates the current correlator to the value of the gauge field at the boundary of the bulk 3+1D spacetime. One then trades the problem of computing two-point functions in a correlated CFT with that of solving Maxwell equations for $A_\mu$ in a specific curved spacetime. The latter contains a (planar) black hole and the $r$-coordinate of the horizon is proportional to the temperature of the boundary CFT. The spacetime tends to $AdS_4$ as $r$ approaches infinity. The gravitational 3+1D Maxwell-Einstein action used to calculate the current correlators of the boundary CFT reads[3]

$$S_{\text{bulk}} = \int d^4x\sqrt{-g}\left[\frac{1}{2\kappa^2}\left(R+\frac{6}{L^2}\right)-\frac{1}{4g_4^2}F_{ab}F^{ab}\right], \tag{15}$$

where $g$ is the determinant of the metric $g_{ab}$ with Ricci scalar $R$; $F^{ab}$ is the field strength tensor of the probe U(1) gauge field $A_a$, where roman indices run over the bulk spacetime components, $(t,x,y,r)$. $L$ is the radius of curvature of the $AdS_4$ spacetime while the gravitational constant $\kappa^2$ is related to the coefficient of the two-point correlator of the stress-energy tensor $T_{\mu\nu}$ of the boundary CFT (this is reviewed in Ref. 30 for e.g.), an analog of the central charge of CFTs in 1+1D. The gauge coupling constant $g_4^2 = 1/\sigma_\infty$ dictates the infinite-$w$ conductivity.

In the absence of the gauge field, which is here only a probe field used to calculate the linear response, the metric that solves the gravitational EoM associated with $S_{\text{bulk}}$ is:

$$ds^2 = \frac{r^2}{L^2}\left(-f(r)dt^2+dx^2+dy^2\right)+\frac{L^2dr^2}{r^2f(r)}, \tag{16}$$

where $f(r) = 1-r_0^3/r^3$. Such a metric describes a spacetime with a planar black hole whose event horizon is located at $r=r_0$ and singularity at $r=0$, and that asymptotically tends to $AdS_4$ as $r\to\infty$. The position of the event horizon is directly proportional to the temperature of the boundary CFT,

$$T = \frac{3r_0}{4\pi L^2}. \tag{17}$$

As $T\to 0$, the black hole disappears and we are left with pure $AdS_4$, which is holographically dual to the vacuum of the CFT. The presence of a horizon permits the study of thermal states since the energy that is Hawking radiated from it "heats up the boundary". It will be more convenient to use the dimensionless coordinate $u = r_0/r$, in terms of which Eq. (16) becomes

$$ds^2 = \frac{r_0^2}{L^2u^2}\left(-f(u)dt^2+dx^2+dy^2\right)+\frac{L^2du^2}{u^2f(u)}, \qquad f(u) = 1-u^3. \tag{18}$$

The EoM for the probe gauge field is then the Maxwell equation $\nabla_a F^{ab}=0$, where $\nabla_a$ denotes a covariant derivative with respect to the background metric, $g_{ab}$. As we are interested in the current correlator in frequency-momentum space, we Fourier transform the gauge field:

$$A_a(t,x,y,u) = \int\frac{d^3k}{(2\pi)^3}e^{-i\omega t+i\boldsymbol{k}\cdot\boldsymbol{x}}A_a(\omega,k_x,k_y,u), \tag{19}$$

where the coordinate $u$ was left un-transformed since there is no translational invariance in that direction. We shall

actually solve for the full $u$-dependence of $A_a$. We work in the radial gauge $A_u = 0$. Without loss of generality, we also set the spatial momentum to be along the $x$-direction, $(k_x, k_y) = (k, 0)$. As a result of the self-duality described above, to obtain the full charge response we only need to solve for the transverse correlator $C_{yy} = \Pi^T$. It can be obtained using the AdS/CFT dictionary:

$$\Pi^T(w,q) = -\chi_0 \frac{\partial_u A_y}{A_y}\bigg|_{u=0}, \tag{20}$$

where $A_y$ is the transverse gauge mode with 3-vector $(w, q, 0)$. The explicit EoM for $A_y$ is[3]

$$A_y'' + \frac{f'}{f}A_y' + \frac{w^2 - q^2 f}{f^2}A_y = 0 \tag{21}$$

where primes denote $u$-derivatives. Note that we are using the rescaling introduced above for the frequency and momentum, Eq. (13). To obtain the retarded correlator, we apply an in-falling boundary condition for the waves at the horizon and solve the equation numerically[3,4,10].

In the next section, we examine the frequency-momentum dependence of these correlators in detail.

### B. Familiar behavior of the current correlators

Before looking into the QNMs of the current correlators, which correspond to complex frequencies in the LHP, we first study their behavior at real frequencies. This has been previously done using the AdS/CFT correspondence in Ref. 3. We briefly review the results and make some new observations.

The numerical solution can be found in Fig. 1, where the real and imaginary parts of $C_{tt}$ and $C_{yy}$ are shown in the $(w, q)$ plane. A salient feature is that the real parts of $C_{tt}$ and $C_{yy}$ seem to be mirror images of the imaginary parts with respect to the $w = q$ line. This is shown more clearly in Fig. 2, where the red dashed lines show the real part reflected along the $w = q$ line, $-\Re C_{yy}(q, w)$. The agreement is excellent away from the region $w \sim q$. Further, the real parts of both $C_{tt}$ and $C_{yy}$ are finite mainly in the region $q > w$, while the imaginary parts have support mostly in the complementary region, $w > q$. We note that the above properties, that are only approximately true here, are *exactly* satisfied by the zero temperature Lorentz invariant correlators, $C_{yy} = \Pi^T = -\sigma_\infty\sqrt{-\omega^2 + k^2}$ and $C_{tt} = k^2\sigma_\infty/\sqrt{-\omega^2 + k^2}$. In fact, the numerical solution for $\Pi^T$ not only closely resembles $\sqrt{-\omega^2 + k^2}$ but the quantitative agreement is excellent away from the region $\omega \sim q$, as is shown in Fig. 2. As expected, the Lorentz invariant form is a better match at frequencies and momenta greater than the temperature: for e.g., the hydrodynamic limit clearly deviates from Lorentz invariance, namely $\Pi^T \sim iw - q^2$. Nonetheless, we note that the zero temperature form and the finite-$T$ transverse correlator are exactly equal at all frequencies at zero momentum:[3] $\Pi^T(w, 0) = -\chi_0 iw$. Similarly, the agreement between the R-charge correlator $C_{tt}$ and the $T = 0$ form is also good except in the region $w \sim q$, where the latter has a square root divergence while the former has a finite peak. The height of the peak grows with momentum thus approaching the $T = 0$ form. It should be again noted that it is not only the large $w \gg q$ region where the agreement is excellent: when $w < q$, $C_{tt}$ decays very rapidly to zero, the more so as $q$ grows.

We have seen that the finite temperature R-current correlators bear a strong imprint from Lorentz invariance. It is thus not unreasonable to interpret them as "smoothed" versions of the zero temperature relativistic forms. For example they show very similar behavior under the exchange of $w$ and $q$, and a similar distribution of spectral weight. As we will see below, the branch cuts of the $T = 0$ forms can be argued to transform into the infinite sequence of poles and zeros present at finite temperature, the QNMs.

### C. Dispersing quasinormal modes

A deeper insight into the physics encoded in the current correlators can be gained by examining their behavior in the complex frequency plane. The finite momentum correlators are meromorphic functions with a discrete set of

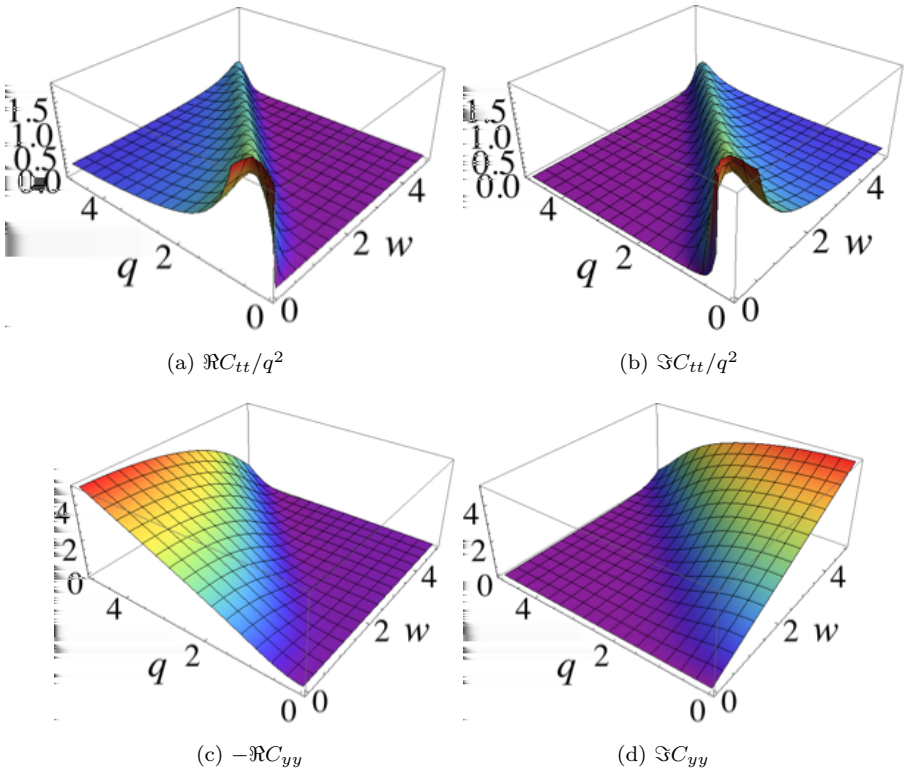


(a) $\Re C_{tt}/q^2$ (b) $\Im C_{tt}/q^2$

(c) $-\Re C_{yy}$ (d) $\Im C_{yy}$

FIG. 1. Frequency and momentum dependence of the longitudinal and transverse R-current correlators, $C_{tt}$ and $C_{yy}$, respectively, normalized by $-\chi_0$. Note the reflection property under exchange of $w$ and $q$, a remnant from the Lorentz invariant $T = 0$ form.

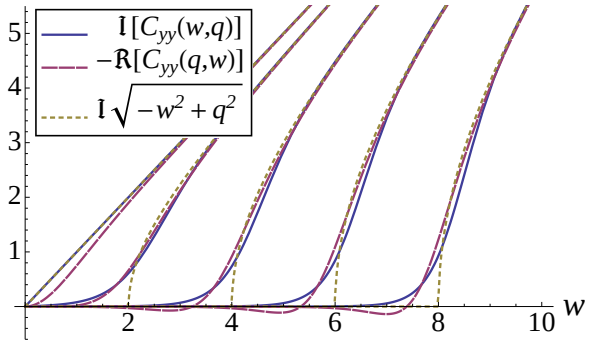


FIG. 2. Comparison of $\Im C_{yy}(w,q)$ with the zero temperature form $\sqrt{-w^2+q^2}$. From left to right: $q = 0, 2, 4, 6, 8$. The plots of $C_{yy}$ are in units of $-\chi_0$. The plot of $-\Re C_{yy}(q,w)$ (note the arguments are interchanged) illustrates the "reflection property".

poles and zeros in the LHP. These correspond to certain QNMs of the black hole in the dual gravitational description. To some extent they replace the quasiparticle excitations of weakly interacting theories, which are clearly lacking for the $\mathcal{N} = 8$ correlated CFT of interest. In the following we discuss how these QNMs disperse as a function of momentum, and how this can help quantify hydrodynamic-to-relativistic crossovers. The essential features of the QNM spectrum have been identified in previous works[31,32]. Our analysis not only corroborates these results but we make further new observations. This will also serve as a comparison ground for Section IV, where we study more general holographic actions. We also mention that Refs. 33 (3+1D) and 34, 35 (2+1D) have studied closely related phenomena in holographic models for *doped* CFTs at finite temperature, and have made connections between hydrodynamic-to-collisionless crossovers and transitions in the QNM spectrum.

We recall that the poles and zeros of the transverse correlation function $C_{yy}(w,q) = \Pi^T$ determine the entire

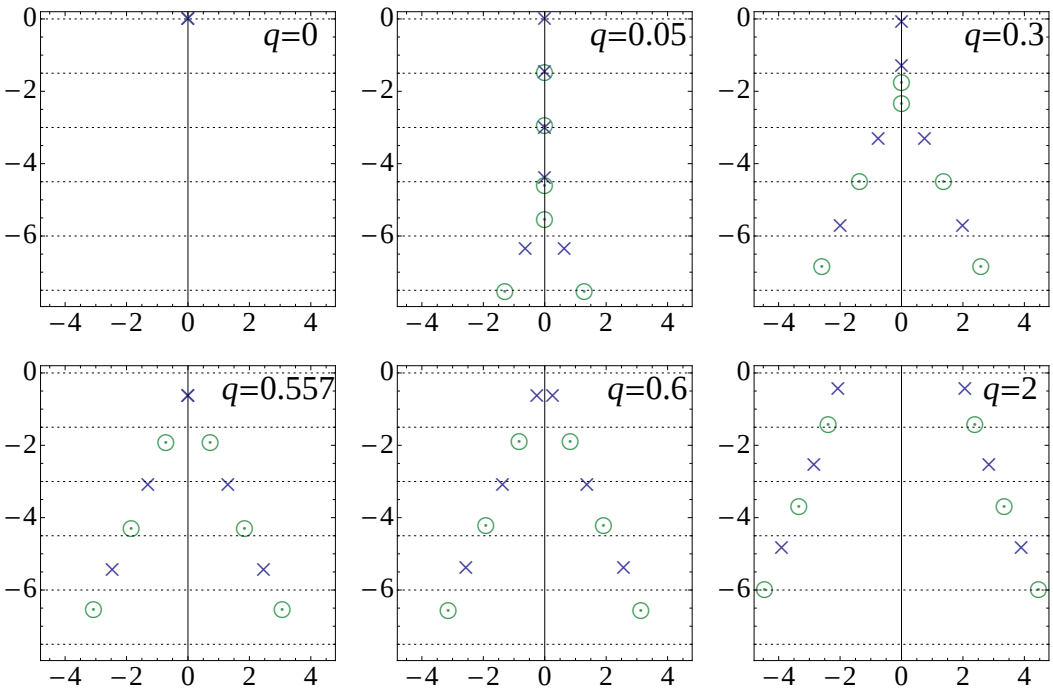


FIG. 3. Poles (crosses) and zeros (circles) in the lower-half complex frequency plane of $C_{tt} = -\chi^2 q^2/\Pi^T(w,q)$, the R-charge density correlation function of the $\mathcal{N}=8$ supersymmetric Yang-Mills CFT. The positions of the poles and zeros are interchanged for $C_{yy} = \Pi^T$.

meromorphic structure of the current correlators because of the EM duality enforcing $\Pi^L = \chi_0^2(-w^2+q^2)/\Pi^T$. From Eq. (20), which states that $\Pi^T = -\chi_0 \partial_u A_y(u=0)/A_y(u=0)$, we see that the frequencies and momenta at which $A_y(u=0)$ vanishes correspond to the poles of $\Pi^T(w,q)$. Equivalently, the zeros of $\partial_u A_y(u=0)$ give the zeros of $\Pi^T$. EM duality then gives the poles and zeros for $C_{tt}(w,q) \propto 1/\Pi^T$, as the zeros and poles of $\Pi^T$, respectively. The low lying poles and zeros can be found using a variety of different methods. Most crudely, one can use the direct numerical solution to the EoM, but this turns out to be unstable as one probes frequencies deeper in the LHP. Alternatively, in Appendix B we provide a solution for the correlators in terms of the local Heun function and its derivative. As no closed-form of its series representation is generally known, and many of its properties are still under study, we were not able to use it to obtain the QNM spectrum. Notwithstanding, its series representation, for which we give the recursion relation, can be useful to obtain a solution when the direct solution of the ODE fails. We mainly resort to a method that focuses on the QNM spectrum specifically. It consists in expanding $A_y$ in a Taylor series in the radial coordinate $u$, being careful to impose the correct asymptotics at the horizon, and especially at the UV boundary, $u=0$, where we require $A_y$ to vanish. We then transform the EoM into a homogeneous matrix equation and ask for values of $(w,q)$ at which it has a solution (by finding the points at which one of the eigenvalues vanishes for e.g.). These are the locations of the QNMs. For further details, see Ref. 4.

The poles and zeros of $C_{tt}(w,q)$ are shown in the LHP of frequency in Fig. 3 for six different momenta. At zero momentum, from the exact solution we know that $\Pi^T(w,0) = -i\chi_0 w$, so that $C_{tt}$ has a single pole at the origin. This is the so-called *hydrodynamic pole*. As momentum is turned on, it disperses quadratically, $w = -iq^2$, as we illustrate in Fig. 5. This is the hallmark of diffusive behavior.[36] The coefficient of $-iq^2$ is precisely 1. Indeed, in terms of the unscaled variables, the dispersion relation reads $\omega = -iD_0 k^2$, where $D_0 = 3/4\pi T$ is the charge diffusion constant and $(w,q) = (\omega,k) \times D_0$. It is the most important QNM of $C_{tt}$ as long as it remains bound to the imaginary axis, i.e. when $q \leq q_c = 0.5573187$, because in that case it is the QNM with the smallest absolute value of the imaginary part, hence it gives the correlation function its dominant, i.e. largest, decay time-scale: $\sim 1/T|\Im w_{\rm QNM}|$.

Another important phenomenon occurs at $q \sim 0^+$: pairs of simple poles and zeros nucleate on the imaginary $w$-axis

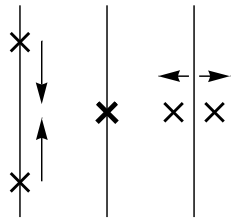

FIG. 4. General mechanism according to which two poles detach from the imaginary axis. A double pole exists at the intermediate step. The same mechanism applies to zeros.

in the immediate vicinity of the frequencies

$$w_n^{\rm zip} = -i3n/2\,, \tag{22}$$

where $n$ is a positive integer. For the unscaled frequency, $\omega = 4\pi T/3$, these correspond to the negative bosonic Matsubara frequencies, $\omega_n^{\rm zip} = -2\pi n T$. As discussed in Appendix B, they correspond to known singular points of the local Heun function, the special function that solves the EoM for $A_y$. From Fig. 3, we see that, with the exception of the special hydrodynamic pole, the nucleation ensures that each pole of $C_{tt}$ comes with a corresponding partner zero, which is a pole for the transverse response function $C_{yy}$. As the momentum is increased from zero, all these QNMs "unzip" from the imaginary axis as is shown in Fig. 3. The unzipping procedure follows the simple rule: 2 poles/zeros join on the imaginary axis to make a double pole/zero, and can subsequently detach. This elementary mechanism, which is illustrated in Fig. 4, is strongly constrained by time-reversal symmetry, which requires the poles and zeros to be distributed symmetrically about the imaginary axis. A related important property of the zeros and poles is their ordering (according to their norm): 2 consecutive poles are followed by 2 consecutive zeros, seemingly *ad infinitum*. We note that a double pole/zero is a superposition of 2 simple poles/zeros and as such respects the ordering property. In Appendix A, we substantiate the claim according to which double poles or zeros, and not higher order ones, occur in the unzipping process. We have observed[4] the same "unzipping" phenomenon in the study of the QNMs of the conductivity in the four-derivative holographic model which we discuss below. In that case, the so-called $\gamma$-coupling plays a role analogous to momentum here. We indeed expect such a phenomenon to be quite general as the poles and zeros must be created/destroyed in pairs.

We observe that it is not only the hydrodynamic QNM that disperses quadratically with momentum but all the zeros and poles do as well, for sufficiently small $q$. Numerical evidence for this is presented in Fig. 12 in Appendix A. Here the smallness condition requires the pole-zero pair emanating from a given frequency $w_n^{\rm zip}$ to be bound to the imaginary axis. The "dispersion relation" for a pair associated with $w_{n>0}^{\rm zip}$ is:

$$w = w_n^{\rm zip} \pm i\alpha_n q^2\,, \quad q \ll 1\,, \tag{23}$$

where $\alpha_n > 0$, and $\alpha_0 = 1$ as stated above. We have found that the dispersion coefficients increase exponentially with $n$ to good accuracy for $n \geq 2$: $\alpha_n \approx a_1 e^{a_2 n}$, where $(a_1, a_2) \approx (0.27, 1.7)$. This leads to the "unzipping" process to occur exponentially fast as momentum is increased from zero so that the QNMs acquire a finite real part very rapidly, as can be observed in Fig. 3.

### 1. *Hydrodynamic-to-relativistic crossover*

The motion of the QNMs can be used to identify the crossover from hydrodynamic-like behavior to a relativistic one. (Note that we use the designation "relativistic" instead of "collision-less", which is sometimes employed, because the latter could suggest the presence of well-defined quasiparticles interacting with each other whereas such a picture does not hold for the strongly correlated theories we describe.) Let us examine the charge density correlator $C_{tt}$. For fixed momentum $q$, $-\Im C_{tt}/q^2$ has a peak at a frequency $w_{\rm max}(q)$, as is illustrated in Fig. 1(b). It was previously

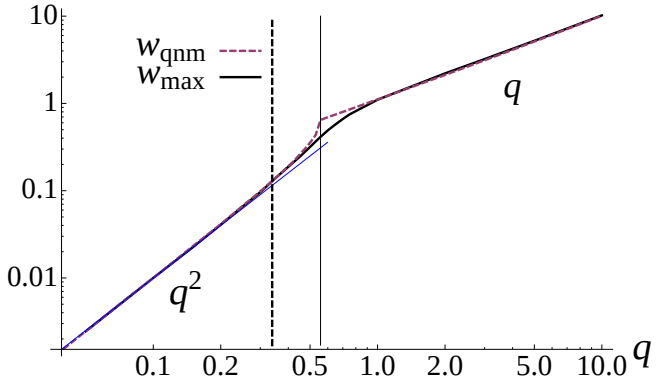


FIG. 5. Hydrodynamic-to-relativistic crossover. Momentum dispersion of the position of the peak of $C_{tt}(w,q)$, $w_{\rm max}(q)$, and the norm of the diffusive QNM, $w_{\rm qnm}(q)$. A quadratic hydrodynamic scaling is seen at small $q$ (as a guide, the thin blue line is $q^2$), while a linear relativistic scaling emerges at large $q$. The vertical lines at $q = 0.339$ and $q = 0.557$ signal momenta at which pairs of QNMs detach from the imaginary axis. The second one is where the diffusive QNM detaches.

observed[3] that $w_{\rm max}(q) \sim q^2$ at small momentum $q \ll 1$, while it scales linearly for $q \gg 1$, see Fig. 5. This signals a crossover from a hydrodynamic behavior at small $q$ to a relativistic one at large $q$. We observe that this crossover corresponds to sharp transitions in the QNM configuration. Namely, from Fig. 5 we find that when the momentum reaches $q \approx 0.33$, the location of the peak starts to noticeably deviate in excess from $q^2$. In the LHP, this actually corresponds to the point where a pair of zero QNMs detaches from the imaginary axis, which occurs at $q = 0.339328$. Next, the scaling for $w_{\rm max}(q)$ has an inflection point near $q \approx 0.6$ after which it rapidly becomes linear. Now, this can be put in correspondence with the momentum at which the diffusive QNM detaches itself from the imaginary axis, which occurs at $q = 0.5573187$. We further find that the value of $w_{\rm max}(q)$ agrees very well with the norm of the lowest lying QNM away from the transition region, $q \approx 0.557$, as Fig. 5 testifies.

Again, just as the diffusive scaling $q^2$ held true for all the QNMs at sufficiently small momentum, so does the linear scaling for $q > 1$. Indeed, the absolute value of the real part of the QNMs grows linearly with increasing momentum, as expected for the low temperature excitations of a CFT. Moreover, the imaginary part of all the modes approaches zero; we illustrate this for the one closest to the real axis in Fig. 13. In Appendix A, we discuss the rate at which this happens as a function of $q$, which for the mode closest to the real axis seems to occur slower than $1/q^{1/4}$. Nevertheless, the lifetime (the inverse of the imaginary part), becomes much less than the excitation energy (real part) at large momenta, and we can thus interpret the QNMs as quasiparticle-like. We also remark that the distance or spacing between theses QNMs decreases as $q$ grows. It is thus suggestive that the QNMs evolve towards the formation of branch cuts, which exist at $T = 0$ due to the form $C_{tt} \propto 1/\sqrt{-w^2+q^2}$. It should be noted that the QNM spectrum has poles closest to the real axis, and these would precisely become the branch poles at zero temperature.

## IV. GENERAL RESPONSE: BEYOND EINSTEIN-MAXWELL

We now turn to holographic models which do not possess EM duality, and as such have independent transverse and longitudinal responses, as is expected for generic CFTs. The role of four-derivative terms in the gravitational action on the charge response was previously considered[9,10] in an effective field theory spirit. The corresponding terms were considered at finite, non-perturbative coupling, in which case the resulting action cannot be interpreted as describing a precise deformation of the original $\mathcal{N} = 8$ Yang-Mills gauge theory. One expects that at finite t'Hooft coupling, $\lambda$, corrections to the $\lambda = \infty$ limit will include higher-derivative corrections in the gravity side, such as the one we consider. However, considering finite 4-derivative couplings in that context would also entail the need to look at higher order terms as well, potentially an infinite tower of them. We adopt an effective approach, considering a truncated action with phenomenological couplings parametrizing all symmetry-allowed terms with a fixed number of derivatives. Based on symmetry, and comparisons with calculations on the CFT side[4], we expect this approach to

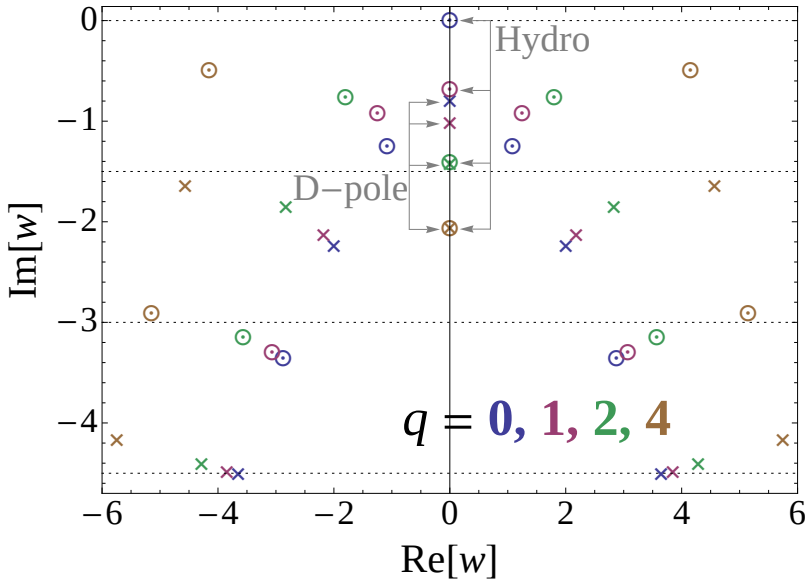


FIG. 6. QNM dispersion of $C_{yy} = \Pi^T(w,q)$ for $\gamma = 1/12$: the crosses/circles represent poles/zeros. The $q = 0$ case gives the QNMs of the conductivity $\sigma(w)$, in addition to the hydrodynamic zero at the origin. The D-pole is the special purely damped QNM giving rise, at $q = 0$, to the DS peak in the small-frequency optical conductivity.

capture some salient properties of the correlators.

It was found that in order to observe non-trivial effects on the correlation function of a single U(1)-current, the only[37] four-derivative term that needs to be added to the Einstein-Maxwell theory studied in the previous section, Eq. (15), while preserving time-reversal is

$$-\int d^4x\sqrt{-g}\,\gamma\frac{L^2}{g_4^2}C^{abcd}F_{ab}F_{cd}\,, \tag{24}$$

where $C$ is the conformal Weyl tensor, the traceless part of the Riemann tensor, and $\gamma$ a dimensionless coupling that was argued to be bounded to $|\gamma| \leq 1/12$ (we refer to Ref. 10 and references therein for a detailed discussion/derivation of the bounds). It was shown that such a term can lead to non-trivial and generic behavior of the conductivity in contrast to the $\gamma = 0$ frequency-independence. In particular, when $\gamma > 0$ ($< 0$) the frequency dependent charge conductivity is particle-like (vortex-like), with the real part showing a peak (valley) near zero frequency. As the Weyl tensor vanishes in pure AdS, this term disappears in the $T \to 0$ limit, and will thus not affect the correlators in the relativistic limit of $\omega, k \gg T$. For instance, the $T = 0$ conductivity $\sigma_\infty = 1/g_4^2$ is independent of $\gamma$, taking the same value as in the $\gamma = 0$ theory.

At finite $\gamma$, the EM self-duality is absent and an EM duality-transformation leads to a non-trivial action on the theory, which should manifest itself as S-duality in the boundary CFT. The action on the gravitational theory is as follows[10]: one introduces a term $\frac{1}{2}\varepsilon^{abcd}\hat{A}_a\partial_b F_{cd}$ to the Lagrangian, and a functional integral over $\hat{A}_a$. $\varepsilon^{abcd}$ is the fully antisymmetric tensor. Such an addition leaves the partition function invariant since the gauge field satisfies the Bianchi identity $\varepsilon^{abcd}\partial_b F_{cd} = 0$. Integrating out the original gauge field yields a new action for $\hat{A}_a$, which has field strength $\hat{F}$:

$$\hat{S}_{\rm bulk} = \int d^4x\sqrt{-g}\left(-\frac{1}{8\hat{g}_4^2}\hat{F}_{ab}\hat{X}^{abcd}\hat{F}_{cd}\right)\,, \tag{25}$$

where the tensor $\hat{X}_{ab}{}^{cd} = -\frac{1}{4}\varepsilon_{ab}{}^{ef}(X^{-1})_{ef}{}^{gh}\varepsilon_{gh}{}^{cd}$ characterizes the bulk action for the dual gauge field just as $X$ does for $A_a$: $X^{abcd}$ simply gives the original action with the Maxwell term and the additional four-derivative $\gamma$-term, Eq. (24). The conductivity obtained from the EM-dual gravitational description gives rise to a conductivity that is

the inverse of the original one, $\hat{\sigma} = 1/\sigma$, where $\sigma$ is the full complex conductivity. This is analogous to what happens under particle-vortex duality in the O(2) model for instance. It was shown[10] that one can relate the current correlators of the original and S-dual theories as follows:

$$\Pi^L(w,q)\hat{\Pi}^T(w,q) = \chi_0\hat{\chi}_0(-w^2+q^2)\,, \tag{26}$$
$$\hat{\Pi}^L(w,q)\Pi^T(w,q) = \chi_0\hat{\chi}_0(-w^2+q^2)\,, \tag{27}$$

where the hats denote the S-dual correlators, and $\chi_0\hat{\chi}_0 = (4\pi T/3g_4^2)(4\pi T/3\hat{g}_4^2) = (4\pi T/3)^2$ since $\hat{g}_4 = 1/g_4$. The above two relations relate the transverse response of the original theory to the longitudinal response of the S-dual one and vice-versa. In particular, the poles and zeros of $\Pi^{L,T}$ map to the zeros and poles of $\hat{\Pi}^{T,L}$, respectively. Further, all the information is contained in the two transverse correlators $\Pi^T$ and $\hat{\Pi}^T$, which we found the easiest to compute given the similarity between the EoMs of $A_y$ and its EM dual, $\hat{A}_y$. The modified Maxwell equations that we need to solve are $\nabla_b(X^{abcd}F_{cd}) = \nabla_b(F^{ab} - 4\gamma L^2 C^{abcd}F_{cd}) = 0$, and $\nabla_b(\hat{X}^{abcd}\hat{F}_{cd}) = 0$, and they lead to the following EoMs for the transverse gauge field and its EM dual[10]:

$$A_y'' + \left(\frac{f'}{f} + \frac{g'}{g}\right)A_y' + \frac{w^2 - q^2 f(1-8\gamma u^3)/g}{f^2}A_y = 0\,, \tag{28}$$
$$\hat{A}_y'' + \left(\frac{f'}{f} + \frac{g'}{g}\right)\hat{A}_y' + \frac{w^2 - q^2 fg/(1-8\gamma u^3)}{f^2}\hat{A}_y = 0\,, \tag{29}$$

where $g(u) = 1 + 4\gamma u^3$. They both reduce to Eq. (21) when $\gamma = 0$, in agreement with self-duality.

#### *2. Sign of $\gamma$ and EM/S-duality*

From the observations made above we can draw a connection between the sign of $\gamma$ and the action of EM duality on the bulk action, and the corresponding S-duality on the boundary. It was previously noted[4,10] that for $|\gamma| \ll 1$, the action of the EM duality described above is tantamount to changing the sign of $\gamma$. (We note that the inversion of the bulk gauge coupling $g_4 \to g_4^{-1}$ is of little importance to our discussion.) This agrees with the particle- and vortex-like conductivities at $\gamma > 0$ and $\gamma < 0$, respectively. For general $|\gamma| \leq 1/12$, this correspondence qualitatively holds although the quantitative agreement deteriorates with increasing $|\gamma|$. Notwithstanding, the conductivity will invariably have a purely imaginary pole for $\gamma > 0$ and a zero when $\gamma$'s sign is reversed. We designate these as D-QNMs due to their purely damped nature as well as their formal relation to the standard Drude form for the optical conductivity.

### A. Finite $\gamma$ QNMs

Let us first examine the QNMs of $C_{yy} = \Pi^T(w,q)$ in the particle-like theory at $\gamma = 1/12$, as shown in Fig. 6. At $q = 0$, this is precisely the meromorphic structure of the conductivity $\sigma(w) = iD_0\Pi^T(w,0)/w$, with the addition of the hydrodynamic zero at the origin, which is annihilated by the factor of $1/w$ in the expression for the conductivity. An important difference with the $\gamma = 0$ case discussed above (Fig. 3) is that even at $q = 0$, $\Pi^T$ already has a sequence of poles and zeros lying away from the imaginary axis. Another important difference is the presence of a pole directly on the imaginary axis at $w_{\rm D}(q=0) = -i0.821075$, this is the D-pole of the conductivity discussed previously[4,22]. Such a pole is absent in the $\gamma = 0$ self-dual theory and alters the QNM spectrum in an essential way. In particular, it can lead to a different kind of crossover in the spectrum compared with the $\gamma = 0$ theory. However, before discussing the intermediate crossover regime, $q \sim 1$, let us examine what happens at small momenta $q \ll 1$.

### B. Hydrodynamic zero and S-dual diffusion constant

As the momentum $q$ is increased from 0, both the hydrodynamic zero and the D-pole will move down the imaginary axis. Already at $q = 2$, they are almost on top of each other (Fig. 6), and as momentum is increased they further move down as a tightly bound pair. At small momentum, the hydrodynamic zero disperses as $w = -i0.625q^2$ while the D-pole as $w = w_{\rm D}(q = 0) - i0.2264q^2$. It is interesting to note that since the hydrodynamic zero disperses faster than the D-pole, they will eventually fuse (at which point they momentarily disappear) and then move through each other. This happens when $q \approx 2.1215$, and the crossing or fusing frequency is found to be precisely the first zipping point $w_1^{\rm zip} = -i3/2$. We now take a closer look into the small momentum dispersion of the hydrodynamic zero.

We recall Eq. (10), which says that at small frequencies and momenta, the transverse correlator becomes

$$C_{yy}(\omega, k) = -\sigma_{\rm dc}(i\omega - \hat{D}k^2)\,, \tag{30}$$

where $\hat{D}$ is the charge diffusion constant of the S-dual theory; $\sigma_{\rm dc} = (1 + 4\gamma)g_4^{-2}$ is the d.c. conductivity[10]. The appearance of the S-dual diffusion constant and not $D$ can be seen to arise from Eq. (27), which relates the transverse response to the inverse longitudinal response of the S-dual theory. As mentioned above, the dispersion of the zero has yielded $\hat{D}/D_0 \approx 0.625$, which is close but not equal to $D_0/D(\gamma = 1/12) = 0.579$, so that $\hat{D} \neq 1/D$ and the relation between the diffusion constants (and hence the susceptibilities) is not as simple as that between the d.c. conductivities. As matter of fact, $\hat{D}$ is closer to $D(\gamma = -1/12) = 0.585D_0$.

We can use the extension[38,39] of the membrane paradigm[40] adapted to our gravitational action to determine the actual diffusion constant of the S-dual theory. The general idea is to consider a stretched horizon located at $r_s$, with $r_s > r_0$. One then combines the stretching-direction 4-vector $n_\mu = (0, 0, 0, g_{rr}^{1/2} r_s)$ with the field strength to form a conserved current, $j^\mu = n_\nu F^{\mu\nu}$. The conservation law for the latter can be recast as a diffusion equation, $\partial_t j^0 = \hat{D}\partial_i\partial_i j^0$, where $\hat{D}$ is the charge diffusion constant we seek. Adapting the expression[10] for the diffusion constant to the dual theory we get

$$\hat{D} = D_0\sqrt{-g}\,\sqrt{-\hat{X}^{xtxt}\hat{X}^{xuxu}}\Big|_{u=1}\int_0^1 \frac{du}{\sqrt{-g}\hat{X}^{tutu}}\,, \tag{31}$$

where the tensor $\hat{X}$ describes the action for the dual gauge field, as introduced in Eq. (25). From Ref. 10 we have $\hat{X}_{tx}{}^{tx} = \hat{X}_{xu}{}^{xu} = 1/(1 + 4\gamma u^3)$ and $\hat{X}_{tu}{}^{tu} = 1/(1 - 8\gamma u^3)$. Finally, using our AdS-Schwarzchild metric Eq. (18) we obtain

$$\frac{\hat{D}}{D_0} = \frac{1 - 2\gamma}{1 + 4\gamma}\,. \tag{32}$$

Evaluating this expression at $\gamma = 1/12$, we find $\hat{D}/D_0 = 5/8 = 0.625$, in exact agreement with our above numerical result for the dispersion relation of the hydrodynamic zero of $\Pi^T$. We note that the dual diffusion constant takes a simpler form than in the direct theory, where it reads[10]

$$\frac{D}{D_0} = \frac{1 + 4\gamma}{12\gamma^{1/3}}\left[\pi\sqrt{3} - 2\sqrt{3}\tan^{-1}\left(\frac{1 + \gamma^{1/3}}{\sqrt{3}\gamma^{1/3}}\right) + \ln\left(\frac{1 - 8\gamma}{(1 - 2\gamma^{1/3})^3}\right)\right]\,. \tag{33}$$

One can also apply an Ohm's law to the stretched horizon[9] to recover the S-dual d.c. conductivity:

$$\hat{\sigma}_{\rm dc} = \frac{1}{\hat{g}_4^2}\,\sqrt{-g}\sqrt{-\hat{X}^{xtxt}\hat{X}^{xuxu}}\Big|_{u=1} \tag{34}$$

$$= \frac{g_4^2}{1 + 4\gamma}\,. \tag{35}$$

This agrees with the action of S-duality on the conductivity: $\hat{\sigma} = 1/\sigma$, valid at all frequencies. Finally, using the

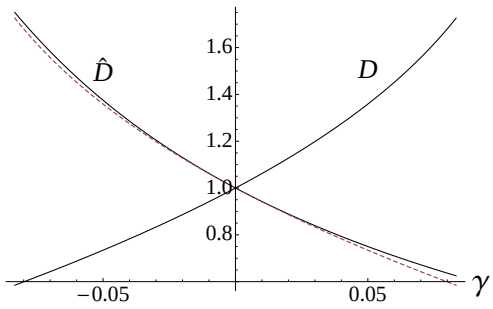


FIG. 7. Diffusion constant, $D$, and its S-dual, $\hat{D}$, in units of $D_0$ for $|\gamma| < 1/12$. The dashed line gives $D(-\gamma)$, which agrees well with $\hat{D}$ at small $|\gamma|$ in accordance with the relation between the sign of $\gamma$ and EM/S-duality. Although not shown, $1/D$ is very close to $D(-\gamma)$ and hence to $\hat{D}$.

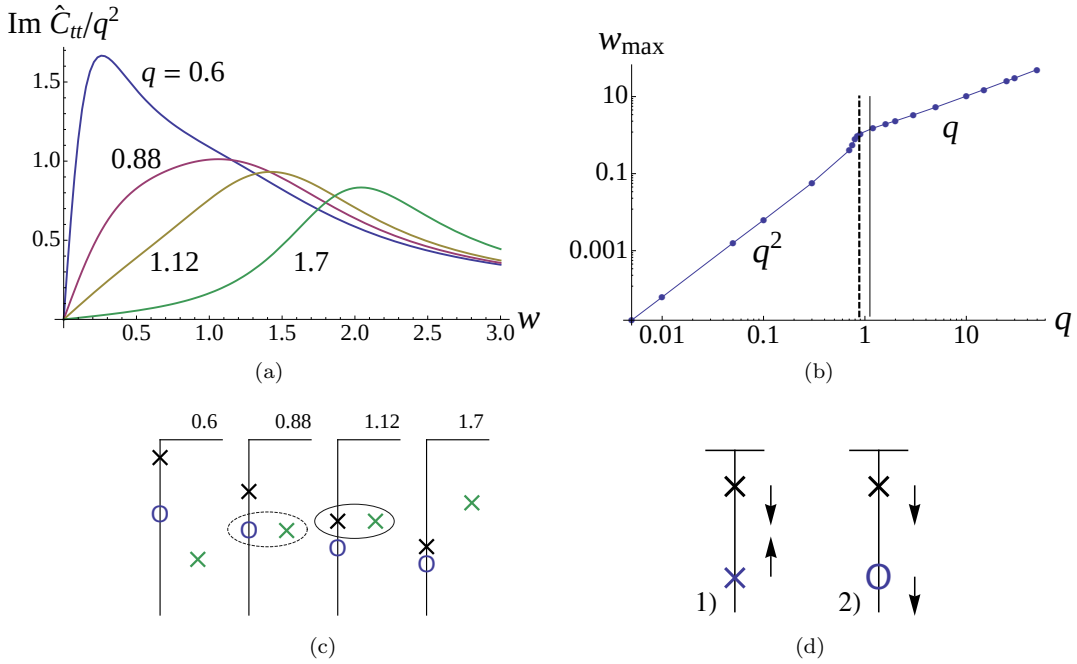


FIG. 8. Hydrodynamic-to-relativistic crossovers at finite $\gamma$. a) $\Im\hat{C}_{tt}(w,q)$ at $\gamma = 1/12$, in units of $-\hat{\chi}_0$, for 4 different momenta. b) Dispersion of the peak of $\Im\hat{C}_{tt}$. The vertical dashed and solid lines correspond to $q_{c1} = 0.88$ and $q_{c2} = 1.12$, respectively. c) The momentum evolution of the 3 QNMs nearest the real axis in the complex $w$-plane ($\Re w \geq 0$ & $\Im w < 0$). Poles are represented by crosses while zeros by circles. d) Two cases for the motion of the hydrodynamic pole and the D-QNM. Case 2 applies to the correlator under study in panels a, b & c. Case 1 applies to $C_{tt}(\gamma > 0)$ for example.

Einstein relation for the S-dual theory, $\hat{D}\hat{\chi} = \hat{\sigma}_0$, we get a simple expression for the S-dual charge susceptibility:

$$\hat{\chi} = \frac{4\pi T g_4^2}{3}\frac{1}{1-2\gamma} \tag{36}$$

### C. Hydrodynamic-to-relativistic crossover

If we examine the behavior of the QNMs away from the real axis, we find that the absolute value of their real part grows with $q$, where for sufficiently large $q$, the increase is linear with momentum, just as we found for the $\gamma = 0$ theory. At the same time, the imaginary part of these propagating QNMs tends to zero. We thus recover

relativistic quasiparticle-like QNMs, and the spectrum evolves towards the asymptotic formation of a pair of branch cuts emanating from the points $w = \pm q$, characteristic of the $T = 0$ form $\sqrt{-w^2 + q^2}$. These phenomena can be observed in Fig. 6. At large momenta, $\gamma$ becomes less important and it is not surprising to recover behavior similar to the $\gamma = 0$ case. We now explain how the diffusive behavior discussed above crosses-over to this relativistic regime.

One of the main results of this section is that the presence of a purely damped *zero*, a D-QNM, at finite $\gamma$ can lead to a transition in the QNM spectrum that is distinct from the $\gamma = 0$ case presented above. We make our point using the longitudinal correlator of the S-dual theory: $\hat{C}_{tt}(w, q) \propto 1/\Pi^T(w, q)$ at $\gamma = 1/12$. We can thus make a connection with the QNM spectrum of $\Pi^T$ given in Fig. 6. We see that the D-pole of $\Pi^T$ becomes a D-zero of $\hat{C}_{tt}$. We plot the corresponding spectral function for four different momenta in Fig. 8(a). The location of the peak scales quadratically with momentum for $q \lesssim 1$, while the scaling becomes linear in the opposite limit. This can be seen more clearly in Fig. 8(b). We also show a sketch of the evolution of the key QNMs of $\hat{C}_{tt} \propto 1/\Pi^T$ in Fig. 8(c), focusing only on the the QNMs nearest the real axis as they dominate the small frequency response. Contrary to the $\gamma = 0$ case, unzipping cannot occur because a pole and zero cannot conspire to detach from the imaginary axis. In principle, they could annihilate but it turns out this does not occur. Instead, we see that the linear or relativistic behavior begins at $q_{c1} \approx 0.88$ where the purely imaginary zero (the D-pole of $\Pi^T$) acquires the same imaginary part as the off-axis pole, see the dashed oval in Fig. 8(c). A secondary crossover occurs at $q_{c2} \approx 1.12$, where the hydrodynamic pole loses its role of dominance (smallest norm of the imaginary part) to the off-axis pole. The latter keeps approaching the real axis while its real part scales linearly with momentum while the purely damped QNMs propagate towards $-i\infty$. We thus roughly see the general principle at play: the hydrodynamic-to-relativistic crossover occurs when the off-axis QNM acquires a greater "lifetime", $1/|\Im w|$, than the hydrodynamic diffusive mode. The presence of the D-mode leads to an intermediate regime, $q_{1c} < q < q_{2c}$, where the hydrodynamic QNM dominates yet a linear scaling of $w_{\max}(q)$ can be seen. In this transitory regime, the response shows a broader peak signaling the competition of two poles as can be seen in Fig. 8(a). We note that it is only for momenta in excess of $q_{2c}$ that an inflection point for $\Im C_{tt}$ appears at small frequencies, allowing for the strong suppression of spectral weight at $w < q$ as momentum increases.

The example above does not cover all possibilities at finite $\gamma$, as there are in fact two cases depending on whether the D-QNM is a pole or zero, as is illustrated in Fig. 8(d). **Case 2** was the subject of the preceding paragraph since the D-QNM of $\hat{C}_{tt}(\gamma > 0)$ is a zero. Generally, case 2 applies to $C_{tt}(\gamma < 0)$ and $\hat{C}_{tt}(\gamma > 0)$. To see this it suffices to remember that $\sigma(w) \propto iwC_{tt}(w, 0)/q^2$, so that D-QNM of the charge correlator arises from the one of the conductivity, and that S-duality changes a D-pole into a D-zero and vice-versa. **Case 1**, on the other hand, agrees with the $\gamma = 0$ theory, with the difference that in the latter situation no D-pole exists but a pole nonetheless appears at $q > 0$ and plays the same role as the D-one in the crossover. More generally, case 1 applies to $C_{tt}(\gamma > 0)$ and $\hat{C}_{tt}(\gamma < 0)$. An important difference outlined in the above discussion is that in case 1 the poles actually detach from the imaginary axis at some momentum, whereas in case 2 they do not. An additional and related difference is that the two QNMs move toward each other in case 1, whereas they move in the same direction in case 2. This will actually cause the crossover to occur earlier, *viz.* at a smaller momentum, in case 1 versus 2 for a fixed value of $\gamma$. For instance, the two poles of $C_{tt}(\gamma = 1/12)$ collide and detach when $q = 0.3280$, which corresponds to the point at which the quadratic scaling of the peak, $w_{\max} \sim q^2$, starts crossing-over to a linear one. Note that this is almost three times less than the value of the critical momentum of $\hat{C}_{tt}(\gamma = 1/12)$ discussed above (case 1), where we it was found that $q_c \approx 0.9$. The same conclusion can be drawn for $\hat{C}_{tt}(\gamma = -1/12)$, where the unzipping of the hydrodynamic and D-poles occurs at $q = 0.3045$.

## V. SUM RULES AND CAUSALITY

We discuss certain integral relations involving the current correlators for any momentum; these include the conductivity sum rules discussed previously[4,20] as special cases. As is generally the case when one deals with retarded

correlation functions, the sum rules rely on Kramers-Kronig relations, such as

$$\Im\psi(w') = \frac{1}{\pi}\mathcal{P}\int_{-\infty}^{\infty} dw \frac{\Re\psi(w)}{w-w'} \quad \xrightarrow{w'\to 0} \quad \Im\psi(0) = \frac{1}{\pi}\mathcal{P}\int_{-\infty}^{\infty} dw \frac{\Re\psi(w)}{w} \tag{37}$$

where $\psi$ is analytic in the UHP and decays sufficiently fast at infinity. The arrow indicates the zero-frequency limit $w' \to 0$ of this Hilbert transform relation, which will be our main tool below. One subtlety arises because CFTs have an abundance of excitations at all energy scales, namely the appearance of UV singularities. These can be dealt with using the appropriate simple subtractions[4,20].

The first relation is

$$\int_0^{\infty} dw \frac{\Re[i\Pi^T(w,q) - \chi_0 w]}{w} = -\frac{\pi}{2}\Pi^T(0,q)\,, \tag{38}$$

$$q \to 0: \quad \int_0^{\infty} dw[\Re\sigma(w) - \sigma_\infty] = 0\ . \tag{39}$$

We have omitted the principal value in the first equation because the integrand is finite at $w = 0$ since $\Pi(0,q)$ is real; further, the extra factor of $1/2$ on the r.h.s. appears because the integral is over the non-negative frequencies only. The static correlator on the r.h.s. of the first equation is not only real but also positive for $q > 0$. It vanishes identically at zero momentum, $\Pi^T(0,0) = 0$, yielding the conductivity sum rule, Eq. (39). The convergence of the integral in the l.h.s. of Eq. (38) is guaranteed by the fact that the function $\Re[i\Pi^T(w,q) - \chi_0 w]/w$ decays sufficiently fast as $w \to \infty$ and $q$ remains finite, namely as $1/w^2$. Note that this is the slowest integer-power decay compatible with the odd nature of $\Im\Pi^T$. This can be understood by referring to the zero temperature form $-\Im\sqrt{-w^2+q^2}$, to which the finite temperature correlator tends in the $w \gg q$ limit. Its asymptotic expansion is $-w + q^2/2w + \mathcal{O}(w^{-3})$, in accordance with our above claim for the decay of the integrand. We have numerically verified that the coefficient of the subleading term, $q^2/2$, matches the behavior of the full solution. It should be noted that the scaling for $q = 0$ is generically different. When $\gamma = 0$ for instance, the spectral function does not have subleading terms as it scales exactly linearly. For finite $\gamma$, we have numerically found that the subleading term decays faster than $w^{-2}$, although we cannot at this time soundly establish the precise power.

We now discuss the basic physics underlying the conductivity sum rule Eq. (39). As we just saw, the reasons underlying the Kramers-Kronig relation, Eq. (38), are 1) the causal structure of the correlation function (analyticity in the UHP of frequency) and 2) the sufficiently fast decay of the integrand at large frequencies essentially due to Lorentz invariance. It remains to understand why does the r.h.s. of Eq. (38), $\propto \Pi^T(0,q)$, vanish at zero momentum, leading the conductivity sum rule. One way to see this is to recall that the conductivity $\sigma(w) = i\Pi(w,0)D_0/w$ of the CFT is finite in the d.c. limit due to the particle-hole or charge-conjugation symmetry. As such, $\Pi^T(w,0) \propto -iw$, i.e. it must vanish at zero frequency. Now, can we also make an argument that relies purely on the holographic bulk? We argue to the positive: the sum rule is a manifestation of *gauge invariance of the bulk gauge field*. In the rest of the paragraph, we explain the argument connecting bulk gauge invariance with the vanishing of the transverse correlator at zero frequency and momentum, $\Pi^T(0,0) = 0$. We first recall the AdS/CFT relation $\Pi^T(w,q) = -\chi_0 A_y'(0;w,q)/A_y(0;w,q)$, where primes denote $u$-derivatives. So that $\Pi^T(0,0) = 0$ is equivalent to $A_y'(0;0,0) = 0$, where we have used the fact that $A_y$ remains finite in the limit under consideration. This follows from the existence of a well-behaved hydrodynamic limit for $\Pi^T$. Further, $A_y'$ vanishes in the near-horizon region in the limit of vanishing frequency and momentum as is shown at the end of the paragraph. The EoM for $A_y$ reads $A_y'' + p_1(u)A_y' + p_2(u)A_y = 0$, where crucially $p_2 = 0$ when $w = q = 0$ since by gauge invariance terms without derivatives must vanish (a mass is not allowed). The resulting EoM without $p_2 A_y$ then simply propagates the property $A_y'|_{w=q=0} = 0$ all the way to the UV boundary at $u = 0$, and this proves that $A_y'(0;0,0) = \Pi^T(0,0) = 0$. Gauge invariance of the bulk gauge field was essential in the argument. We now prove our claim according to which $A_y'$ vanishes in the near-boundary region when $w, q \to 0$. Near the horizon $u = 1$ one needs to apply an in-falling boundary condition to solve for the retarded $\Pi^T$: $A_y(u;w,q) = (1-u)^{-iw/3}F(u)$ as $u \to 1$, where $F$ is analytic in the vicinity of the horizon and we have the freedom to set $F(1) = 1$. Taking a derivative of $A_y$ gives: $A_y'(1+\epsilon;w,0) = -i\frac{w}{3}(\epsilon^{-1} + e_1)(-\epsilon)^{-iw/3}$, with $\epsilon = 0^+$ so that $u = 1+\epsilon$ is just outside of the

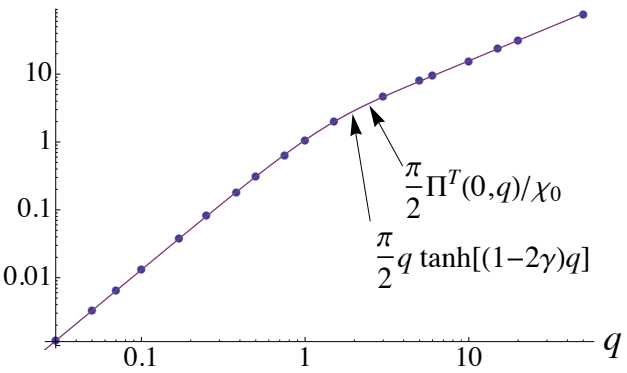


FIG. 9. Verification of sum rule Eq. (38) for $\gamma = 1/12$. The dots correspond to the absolute value of the integral on the l.h.s. of Eq. (38), while the two lines (which cannot be distinguished here) to the static correlator on the r.h.s. of Eq. (38) and its almost exact analytical form.

horizon; $e_1$ is a finite number coming from $F'(1)$. We have used the fact that $F'(1)$ vanishes linearly with $w$ when $q = 0$, which is readily seen to rely on the vanishing of $p_2$ at $w = q = 0$ as guaranteed by gauge invariance[41]. Finally taking the limit $w \to 0$ leads to the desired property. We note that at finite momentum, both $F'(1)$ and the term $p_2(u)A_y$ remain finite as $w \to 0$. This will lead to $\Pi^T(0, q)$ being finite for $q > 0$, and we now turn to study that function in more detail.

We have found that the static correlator obeys the following form to excellent accuracy at all momenta:

$$\Pi^T(0, q) = \chi_0 q \tanh\left(\frac{\hat{\chi}_0}{\hat{\chi}} q\right) \tag{40}$$

where $\hat{\chi}/\hat{\chi}_0 = 1/(1 - 2\gamma)$ is the normalized S-dual charge susceptibility. Not only is the asymptotic behavior exactly captured by that function, the agreement in the crossover region is also excellent, as is shown in Fig. 9. We note that at small momenta the correlator vanishes quadratically, $\Pi^T(0, q) = (\chi_0\hat{\chi}_0/\hat{\chi})q^2 = \chi D\hat{D}k^2$, in agreement with the hydrodynamic form Eq. (30), which also guarantees the conductivity sum rule since $\Pi^T(0, 0) = 0$. At momenta greater than the temperature, the behavior crosses-over rapidly to a linear scaling independent of the S-dual susceptibility. We note that precisely the same form arises for the IR fixed point of the vector O($N$) model in the $N \to \infty$ limit, as will be discussed in the next section (Fig. 11 and Eq. (47)).

The second relation is obtained by taking the S-dual of Eq. (38), with the replacement $\Pi^T(w, q) \to \hat{\Pi}^T(w, q)$:

$$\int_0^\infty dw \frac{\Re[i\hat{\Pi}^T(w, q) - \hat{\chi}_0 w]}{w} = -\frac{\pi}{2}\hat{\Pi}^T(0, q)\,, \tag{41}$$

$$q \to 0: \quad \int_0^\infty dw[\Re\hat{\sigma}(w) - \hat{\sigma}_\infty] = 0\,. \tag{42}$$

In the limit of zero momentum, the S-dual relation Eq. (41) yields the sum rule for the dual conductivity[4], $\hat{\sigma}(w) = 1/\sigma(w)$. The same physical arguments for the sum rule given above apply here as well. Also, we again find an almost exact expression for the static correlator appearing in the r.h.s. of the integral relation: $\hat{\Pi}^T(0, q) \approx \hat{\chi}_0 q \tanh\left(\frac{\chi_0}{\chi} q\right)$. This is the S-dual analog of Eq. (40).

One can also examine another relation that is related to the sum rule for the S-dual conductivity:

$$\int_0^\infty dw \left\{\Re\left[\frac{w}{i\Pi^T(w, q)}\right] - \frac{1}{\chi_0}\right\} = 0 \tag{43}$$

Its proof again follows from the Kramers-Kronig relation Eq. (37) with $\psi(w) = [w^2/i\Pi^T(w, q)] - w/\chi_0$, which vanishes at zero frequency for all momenta, $\psi(0) = 0$, yielding a momentum independent r.h.s to the above equation, contrary

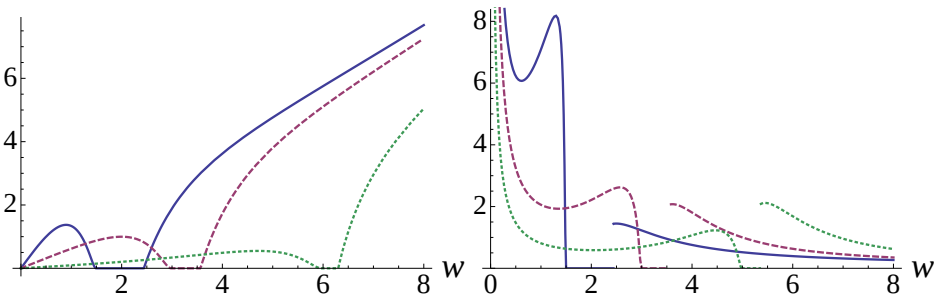


(a) $-\Im C_{yy}$ (b) $-\Im C_{tt}/q^2$

FIG. 10. Quantum critical current correlators of the vector O($N$) model in the $N \to \infty$ limit. They have been normalized by $T\sigma_\infty$, with $\sigma_\infty = 1/16$. From left to right: $q = 1.5$ (solid), 3 (dashed), 6 (dotted).

to Eq. (38) and Eq. (41). The integrand of Eq. (43) again vanishes as $1/w^2$ as can be easily seen using the asymptotic expansion given above: $\Im\Pi^T \propto -w + q^2/2w + \mathcal{O}(w^{-3})$. The real part decays faster and can be safely neglected here. Note that Eq. (43) reduces to the sum rule for the S-dual conductivity, Eq. (42) in the $q \to 0$ limit. Again, the S-dual version also holds and we can use it to establish a sum rule for the spectral density of the charge correlator:

$$\int_0^\infty dw \left\{ -\Im\left[\frac{wD_0^2 C_{tt}(w,q)}{q^2}\right] - \frac{1}{\hat{\chi}_0}\right\} = 0 \tag{44}$$

Finally, we note that although we focused on the zero frequency limit of the Kramers-Kronig relations, they can be used to determine the real part of all the retarded correlators for all frequencies and momenta using the imaginary part, and vice-versa.

## VI. COMPARISON WITH THE O($N$) MODEL

In this section, we compare the current correlators of the vector O($N$) NL$\sigma$M in 2+1D obtained in the large-$N$ limit with the holographic results. It is important to note that we do not claim that such a model has a well-defined classical (super)gravity description as is the case for the $\mathcal{N} = 8$ gauge theory discussed above. This is indeed probably not the case. Rather, we point out that the holographic results capture some essential properties of the current correlators and provide a useful platform to compare with generic CFTs.

The Lagrangian for the vector O($N$) NL$\sigma$M is

$$\mathcal{L} = \frac{1}{2}\partial_\mu \varphi^a(x)\partial^\mu \varphi^a(x)\,, \tag{45}$$

with the constraint $\varphi^a\varphi^a = N/g$, $a = 1, \ldots, N$ and $g$ is the bare coupling. At large but finite $N$, the model has a well-known weakly interacting conformal IR fixed point (for a review and references, see Ref. 1), equivalent to the Wilson-Fisher fixed point accessed by perturbative RG. We study the two-point functions of the conserved $\binom{N}{2}$ currents near the fixed point, mainly in the $N \to \infty$ limit. Just as in the case of the SO(8) R-currents, the correlators are flavor-diagonal and we can focus on a single flavor. In the $N \to \infty$ limit, the fixed point is free, yet shows non-trivial dynamics at finite temperature, see Fig. 10 and the discussion below. The spatial current correlators can be computed using the one-loop polarization functions in the $N \to \infty$ limit (normalized such that $\sigma_\infty = 1/16$):

$$\begin{aligned} C_{ij}(\omega, \boldsymbol{k}) = \int \frac{d^2\boldsymbol{p}}{(2\pi)^2} \frac{p_i p_j}{4\epsilon_p \epsilon_{\boldsymbol{p}+\boldsymbol{k}}} \Bigg\{ & \frac{1 + n(\epsilon_p) + n(\epsilon_{\boldsymbol{p}+\boldsymbol{k}})}{-\epsilon_{\boldsymbol{p}+\boldsymbol{k}} - \epsilon_p + \omega + i0^+} - \frac{1 + n(\epsilon_p) + n(\epsilon_{\boldsymbol{p}+\boldsymbol{k}})}{\epsilon_{\boldsymbol{p}+\boldsymbol{k}} + \epsilon_p + \omega + i0^+} \\ & + \frac{n(\epsilon_{\boldsymbol{p}+\boldsymbol{k}}) - n(\epsilon_p)}{\epsilon_{\boldsymbol{p}+\boldsymbol{k}} - \epsilon_p + \omega + i0^+} + \frac{n(\epsilon_p) - n(\epsilon_{\boldsymbol{p}+\boldsymbol{k}})}{\epsilon_p - \epsilon_{\boldsymbol{p}+\boldsymbol{k}} + \omega + i0^+} - \Re(k \to 0) \Bigg\}\,, \end{aligned} \tag{46}$$

where $\epsilon_k = \sqrt{k^2+m^2}$ and $n(z) = 1/(e^{z/T}-1)$ is the Bose-Einstein distribution. The "mass" parameter is $m = \Theta T$ with $\Theta = 2\ln[(1+\sqrt{5})/2] \approx 0.96$; it corresponds to the temperature-generated mass of the quasiparticles[11]. It is simply the inverse correlation length, and must vanish at the QC point. The subtraction in Eq. (46) is necessary to regulate the UV divergence of the real part. In this section, we use the rescaling $(w,q) = (\omega,k)/T$, without the factor of $3/4\pi$ appearing in the holographic analysis. Just as in the rest of the paper, the momentum is assumed to lie along the $x$-direction.

Let us first examine the transverse correlator $C_{yy}$. It can be numerically evaluated and the result for the imaginary part is shown in Fig. 10(a). The behavior of $C_{yy}(w,q) = \Pi^T$ qualitatively resembles what has been obtained holographically, the more so in the large-$w,q$ limit where both the vector O($N$) and holographic results approach the zero temperature form $\sqrt{-w^2+q^2}$. However, one important "pathology" of the $N=\infty$ limit is the non-meromorphicity of the finite-temperature correlators, which occurs even at finite momentum. Indeed, $\Im C_{yy}$ vanishes identically for $k \leq |\omega| \leq \sqrt{4m^2+k^2}$. The lack of spectral weight in this region is of kinematical origin: the relativistic quasiparticles can absorb/emit energy $\omega$ and momentum $k$ as long as $\omega \leq k$, or they can be created in pairs when $\omega > \sqrt{(2m)^2+k^2}$, the latter being the minimal energy for two quasiparticles of mass $m$ carrying total momentum $k$. Such constraints become irrelevant as interactions appear at $\mathcal{O}(1/N)$ and the spectral weight will thus become finite throughout when $N<\infty$, smoothing out the non-analytic behavior present at $N=\infty$. Although not shown here, the real part of $C_{yy}$ remains finite in the region $k \leq |\omega| \leq \sqrt{4m^2+k^2}$, although non-analytic dependence appears at the upper boundary of that region. In fact, we find that there is a logarithmic branch cut that appears at $\omega_\star = \sqrt{(2m)^2+k^2}$, and at $-\omega_\star$. We have previously identified[4,22] its zero-momentum manifestation in the conductivity, where in addition $\omega_\star = 2m$ becomes a zero of $\sigma = i\Pi^T(\omega,0)/\omega$. At finite but small momentum, $k \ll T$, the branch point disperses quadratically away from its $k=0$ position, $\omega_\star - 2m = k^2/(4m)$, and eventually acquires a relativistic dispersion $\omega_\star = k$, when $k \gg T$. In terms of the real-frequency behavior, both the field theory and holography yield the same small- and large-$w$ asymptotics: $\Im C_{yy} \propto \omega$ in both limits, in agreement with the oddness requirement and dimension of $C_{\mu\nu}$. As momentum tends to zero, the slope of the linear part at small frequencies increases yielding a peak of increasing height for $\Im C_{yy}/w$: this is the formation of the delta function peak of the conductivity obtained in the $q=0$ limit. We have indeed verified that at sufficiently small $q$, the peak rapidly saturates the weight of the $q=0$ delta function. Such behavior is naturally absent in the holographic analysis, where the conductivity of the *interacting* boundary CFT remains finite in the d.c. limit.

We now examine the spectral density of the charge density auto-correlator, $\Im C_{tt}$, which is plotted in Fig. 10(b). Just as $\Im C_{yy}$, it vanishes in the kinematically forbidden region, but now shows a jump discontinuity at the pair-production threshold, $\pm\omega_\star = \pm\sqrt{(2m)^2+k^2}$. This leads to a logarithmic divergence of the real part at $\pm\omega_\star$. The function $\Im C_{tt}(w,q)$ is of course $w$-odd, but instead of vanishing linearly at small frequencies as required by hydrodynamics, it diverges as $1/w$ (in the limit of $q=0$, a double instead of a single pole emerges at the origin so that the real part of the conductivity acquires a delta function). The finite-momentum pole at $w=0$ arises because when $N=\infty$, diffusion does not take place as the theory is free of interactions: the conserved charge must propagate ballistically at all times. At order $1/N$, interactions between the quasiparticles appear and as a consequence so does charge diffusion. The precise value of the large-$N$ diffusion constant, $D = 0.249N/T$, was deduced[1] from the Einstein relation and knowledge of the charge susceptibility[1] and d.c. conductivity[22], which are respectively (to leading order in $1/N$): $\chi = \sqrt{5}\Theta T/2\pi$ and $\sigma_{\rm dc} = 0.085N$. The divergence of the diffusion constant in the $N\to\infty$ limit is in agreement with its interpretation as a scattering time between the critical quasiparticles. In the relativistic limit at large momentum, the spectral function $\Im C_{tt}$ gains resemblance with the $T=0$ form, $1/\sqrt{-w^2+q^2}$, having essentially no weight in the region $w<q$ (except for the $w=0$ pole) and develops a sharp peak at $w\sim q$.

We have seen that at $N=\infty$, the current correlators show branch cuts in the LHP due to the absence of interactions. At finite $N$, we expect the branch points to disappear from the real axis and the spectral weight to spread over all frequencies in line with general expectations, and with the holographic results. One possibility is that the branch cuts split into a discrete sequence of poles and zeros, in analogy with the QNMs that have been discussed above. One such QNM was already found[4,22] at $\mathcal{O}(1/N)$, the D-pole of the transverse correlator, which leads to a pole in the small-frequency conductivity. Another possibility is that the branch cuts move away from the real axis in the LHP.

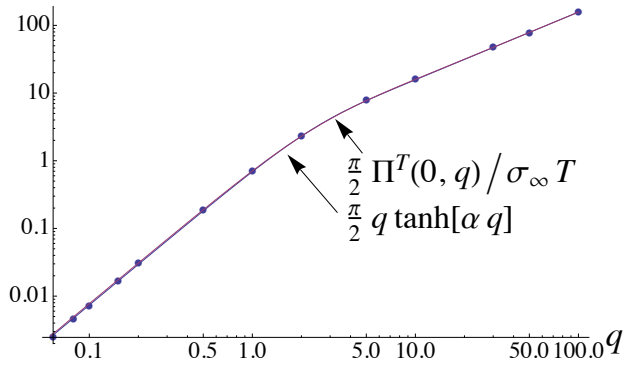


FIG. 11. Verification of sum rule Eq. (38) for the quantum critical vector O($N$) model in the $N \to \infty$ limit. Note the resemblance with the holographic result, Fig. 9.

### A. Sum rule

The $N = \infty$ theory satisfies the sum rule Eq. (38), where the static correlator on the r.h.s., $\Pi^T(0,q)$, can be numerically computed and has precisely the same form as what was found for the holographic models:

$$\Pi^T(0,q) = T\sigma_\infty q \tanh(\alpha q)\,, \tag{47}$$

where $\alpha \approx 0.466$, as we show in Fig. 11. The simplified expression used to calculated the static correlator can be found in Appendix C of Ref. 4. We note that $\alpha$ differs by less than one percent from $T/(2\pi\chi)$, where $\chi = \sqrt{5}\Theta T/2\pi$ as given above. The $q = 0$ version, Eq. (39), i.e. the sum rule for the conductivity was shown to hold previously by us[4]. Just as in the holographic case, we find that $-(\Im\Pi^T/w) - \sigma_\infty$ decays as $1/w^2$ at large frequencies in line with the asymptotic Lorentz invariant form.

## VII. CONCLUSIONS

This paper has described details of the current correlators of CFT3s represented holographically by the Einstein-Maxwell action in Eq. (15), augmented by the Weyl term in Eq. (24). Such an approach has been argued[10] to be the most general representation of the two-point correlator unto 4 derivatives in the holographic theory. In our previous paper[4] we demonstrated that the poles and zeros of the response function identified the quasinormal modes of the holographic theory, and led to a simple and complete description of the frequency-dependent conductivity. These quasinormal modes replace the quasiparticle excitations of a traditional Boltzmann analysis of quantum transport. The present paper has extended such an analysis to spatially modulated response functions, which is linked to the dispersion of the quasinormal modes as a function of momentum.

We refer the reader back to Section I A for a more detailed summary of our results, and focus on the main points here. We have found that the thermal current correlators obtained holographically bear a strong imprint of the $T = 0$ Lorentz invariance, as one can see from the asymptotics and the behavior under exchange of momentum and frequency. Crucially, their QNM spectra were seen to be a useful tool in understanding the nature of the excitation modes of the CFT. For instance, sharp transitions in the QNM distribution were found to correspond to hydrodynamic-to-relativistic crossovers in the real-frequency response functions. In this respect, it was found that the presence of the four-derivative Weyl term can lead to distinct behavior. The two possible cases for the crossover mechanism are epitomized in Fig. 8(d), where in case 1 the hydrodynamic pole and the special purely damped D-pole of the charge correlator, $C_{tt}$, eventually detach from the imaginary axis (Fig. 4), while in case 2, the hydrodynamic pole and D-*zero* cannot detach and instead move down the axis. Case 2 applies to $\gamma < 0$, while case 1 to $\gamma \geq 0$, which includes the pure two-derivative theory describing the R-currents, where although the D-QNM is missing at zero momentum, a

substitute appears for $q > 0$. It was further shown that S-duality, realized as electric-magnetic duality in the bulk, is an integral part of the physics, even for the direct theory. We have finally discussed a number of sum rules generalizing to finite momentum those for conductivity[4,20], some of them in excellent agreement with equivalent statements in the large-$N$ vector O($N$) model. A natural connection between the sum rules and gauge invariance in the holographic bulk was made. It would be interesting to see if such a connection generalizes to other holographic sum rules such as those derived in Ref. 20.

We conclude our discussion by comparing the holographic description of the quantum-critical conductivity to quantum Monte Carlo results on the O(2) critical point obtained some time ago.[42] The O(2) model has[42,43] $\sigma_\infty \approx 0.33Q^2/h$ in the $\omega/T \to \infty$ limit, where $Q$ is the charge of the bosons. The analytic continuation of imaginary time Monte Carlo data gave the estimate for the d.c. conductivity at non-zero temperature of[42] $\sigma(0) \approx 0.45Q^2/h$, which yields the ratio $\sigma(0)/\sigma_\infty \approx 1.36$. The holographic prediction of the four-derivative theory is[10] $\sigma(0)/\sigma_\infty = 1 + 4\gamma$, along with the bound $|\gamma| \leq 1/12$. Interestingly, the maximum possible holographic value at $\gamma = 1/12$ of 1.33 is very close to the current quantum Monte Carlo estimate. This value of $\gamma$ is also consistent with considerations[30] from $T = 0$ multipoint correlators of the CFT3, when computed in a vector large-$N$ expansion of the S-dual conformal gauge theory. In future work, it would be interesting to obtain additional Monte Carlo data which allow comparison with the frequency and momentum dependence predicted by the holographic theory.

## ACKNOWLEDGMENTS

We are grateful to S. Hartnoll and C.P. Herzog for their comments on the manuscript, and to V. Cardoso for discussions regarding the QNM spectrum. The research was supported by the U.S. National Science Foundation under grant DMR-1103860, and by the U.S. Army Research Office Award W911NF-12-1-0227 (S.S.); and by the Walter Sumner Foundation (W.W.-K.). Research at Perimeter Institute is supported by the Government of Canada through Industry Canada and by the Province of Ontario through the Ministry of Research & Innovation.

## Appendix A: Properties of QNMs

In this appendix we discuss various properties of the momentum-dependence of the QNMs of the $\gamma = 0$ theory in more detail.

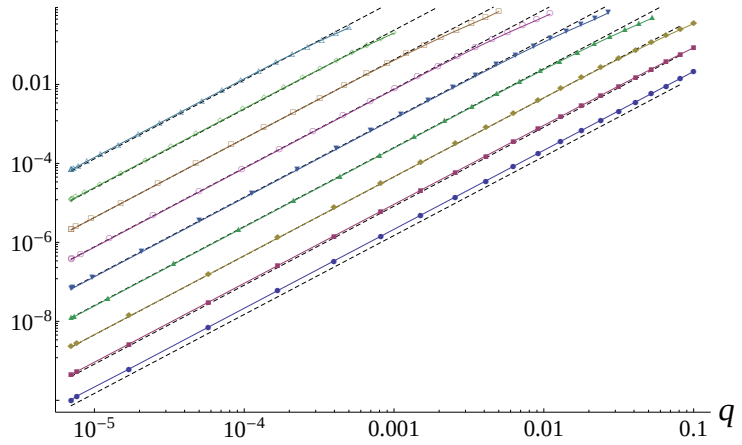


FIG. 12. Momentum dispersion of the first 9 members of the tower of purely damped QNMs that propagate towards $w = 0$. Their real part vanishes, and we plot the imaginary part relative to the zipping point out of which they emerge at $q = 0$: $w_n - w_n^{\rm zip} = i\alpha_n q^2$. From bottom to top: $n = 1$ to 9. The dashed lines are quadratic dispersions with the coefficients satisfying $\alpha_n \approx a_1 e^{a_2 n}$, $(a_1, a_2) = (0.27, 1.71)$.

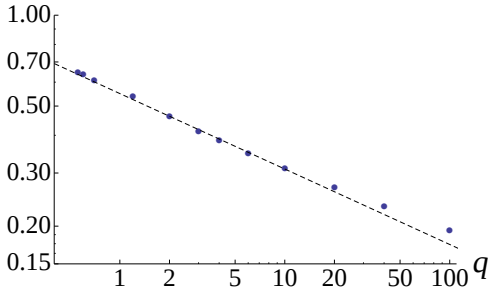


FIG. 13. Absolute value of the imaginary part of the QNM closest to the real frequency axis as function of momentum. The dashed line is $\propto 1/q^{1/4}$.

### 1. Quadratic dispersion

At $\gamma = 0$ and for infinitesimal momentum $q$, all the QNMs of the current correlators appear on the imaginary axis at the special zipping frequencies $w_n^{\rm zip} = -i3n/2$, where $n \geq 0$ is an integer. The diffusive pole of $C_{tt}$ is already present even at $q = 0$. Just as the diffusive pole, all the QNMs, i.e. both poles and zeros of $C_{tt}$, disperse quadratically with momentum away from their respective zipping point. This is shown in Fig. 12, where we only show the QNMs propagating towards zero, $w_n = w_n^{\rm zip} + i\alpha_n q^2$, with $\alpha_n > 0$, with $1 \leq n \leq 9$. The $n = 1$ upward propagating mode is a pole of $C_{tt}$, $n = 2$ is a zero, and so forth. The partner QNMs propagating toward $-i\infty$ disperse as $w_n^{\rm zip} - i\alpha_n q^2$ and are thus not shown for clarity. As discussed in the main body, the dispersion coefficients grow exponentially with $n$. This can be seen form the dashed lines in Fig. 12. In particular, this exponential growth of the dispersion coefficients implies that the unzipping process will occur exponentially fast as $q$ is tuned from zero to 0.557, at which point the last QNMs detach from the imaginary axis.

### 2. Double poles and zeros

In the main body, we described the generic unzipping process that occurs as a function of momentum. It also occurs at zero momentum as a function of $\gamma$ at zero momentum as noted previously[4]. Here we substantiate the claim by plotting the charge density spectral function $-\Im C_{tt}(w, q)$ as a function of momentum. As $q$ changes from $q < q_c$ to $q > q_c$, a double pole appears directly at $q_c = 0.5573187$. As we are plotting the imaginary part of $C_{tt}$ not the norm, the phase structure shows very clearly that we have a double pole at $q_c$, with four lobes, in contrast to single poles that have only two lobes.

### 3. Lifetimes

Still at $\gamma = 0$, we now take a closer look at the rate at which the imaginary part of the QNM closest to the real axis approaches zero. We track the imaginary part of the QNM after it detaches from the imaginary axis at momentum $q_c$ as described in the previous subsection. The result is shown in Fig. 13, where we see that the imaginary part vanishes relatively slowly, slower than $1/q^{1/4}$ in the regime we have investigated. We recall that the absolute value of the imaginary part should correspond to the inverse lifetime of that mode or quasiparticle, while the real part describes its excitation energy. In contrast, the real part scales linearly with momentum.

## Appendix B: Analysis of differential equations

We discuss the underlying structure of the ODEs appearing in the main body, namely those for the transverse gauge field $A_y$, and its EM-dual, $\hat{A}_y$. This sheds some light on the physics and provides an additional mathematical

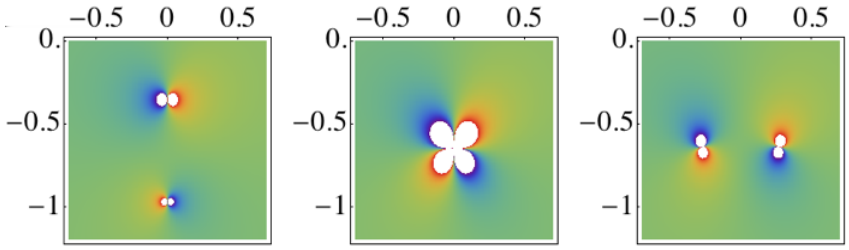


FIG. 14. Formation of a double pole for $C_{tt}(w,q)$ as a function of $q$ at the intermediate step of the unzipping process. Plots of $-\Im C_{tt}$ are in the LHP $w$-plane. Left to right: $q = 0.5, 0.557, 0.6$. Red represents positive values while blue negative ones.

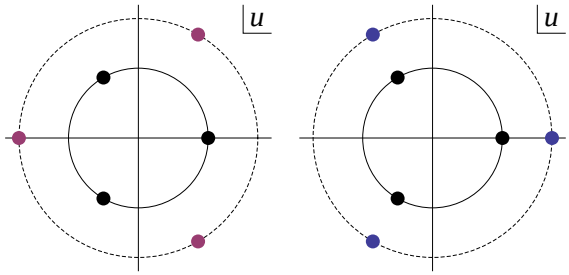


(a) $\gamma > 0$ (b) $\gamma < 0$

FIG. 15. Regular singular points (RSPs), excluding the one at $\infty$, of the EoM of the transverse gauge mode $A_y$ in the complex $u$-plane. The 3 on the inner circle correspond to the horizon, and its 2 complex partners. The outer radius (dashed) has radius $1/(4|\gamma|)^{1/3}$. When $\gamma = 0$, the outer-radius RSPs disappear and only 3 finite RSPs remain.

handle on the problem.

### 1. $\gamma = 0$: Heun's equation

Let us first discuss the $\gamma = 0$ EoM for $A_y(u)$,

$$A_y'' + \frac{f'}{f}A_y' + \frac{w^2 - q^2 f}{f^2}A_y = 0\,, \qquad f(u) = 1 - u^3\,. \tag{B1}$$

It is a *Fuchsian* ODE, namely it is a linear and homogeneous differential equation with a finite number of singular points on the Riemann sphere $\mathbb{C}P^1 = \mathbb{C} \cup \{\infty\}$, all of them *regular*. We are thus including the point at infinity in our treatment. In terms of the coordinate $u = 1/r$, this point corresponds to the black hole singularity at $r = 0$. The above ODE has 4 regular singular points (RSPs): $1, \zeta, \zeta^2 = \zeta^*$ and $\infty$, where $\zeta = e^{-i2\pi/3}$ so that the first 3 RSPs are the cubic roots of unity, the zeros of $f = 1 - u^3$, they are shown on the solid circle of Fig. 15. In the same way that all second order Fuchsian ODEs with 3 RSPs can be mapped to the hypergeometric equation, all the ones with 4 RSPs can be mapped to the so-called *Heun equation*[44,45]:

$$\frac{d^2H}{ds^2} + \left(\frac{\delta_1}{s} + \frac{\delta_2}{s-1} + \frac{\delta_3}{s-a}\right)\frac{dH}{ds} + \frac{\alpha\beta s - Q}{s(s-1)(s-a)}H = 0 \tag{B2}$$

where $\delta_3 = \alpha + \beta - \delta_1 - \delta_2 + 1$. This equation has RSPs at $0, 1, a, \infty$. Our original equation can be mapped to this one via the following simple canonical transformations. First, we perform the linear change of variables:

$$u = (\zeta - 1)s + 1\,. \tag{B3}$$

This maps the RSPs as follows: $1 \to 0$, $\zeta \to 1$, $\zeta^2 \to -\zeta^2 =: a$ and preserves the one at $\infty$. Second, we define:

$$A_y = s^{b_1}(s-1)^{b_2}(s-a)^{b_3}H(s)\,, \tag{B4}$$

where the exponents $b_1, b_2, b_3$ are chosen to remove the terms proportional to $1/s^2$, $1/(s-1)^2$ and $1/(s-a)^2$, respectively, that appear in the transformed equation. The algebraic equations for the $b_i$ are readily found to be:

$$b_i^2 + \frac{w^2}{9}u_i = 0\,, \quad i = 1,2,3\,, \tag{B5}$$

where $(u_1, u_2, u_3) = (1, \zeta, \zeta^2)$ are the RSPs excluding $\infty$. These are precisely the indicial equations of the corresponding RSPs of the original ODE Eq. (B1); their solutions yield the 2 characteristic exponents associated with each RSP. This is not so surprising as the indicial equation at $u_i$ can be obtained by substituting the power law solution $(u-u_i)^{b_i}$ in the ODE Eq. (B1) and solving for $b_i$ in the limit where $u \to u_i$. The solutions of Eq. (B5) are $b_i = \pm iwu_i/3$. We note that Eq. (B5) is not the indicial equation in the new variable $s$, as the latter equation is transformed and the corresponding characteristic exponents differ. The transformation Eq. (B4) shifts both characteristic exponents at each RSP $u_i$ by $-b_i$, and the ones associated with the RSP at $\infty$ by $b_1 + b_2 + b_3 = 0$.

Fixing the $b_i$ as we have just described yields the desired form; it only remains to read off the Heun parameters. The resulting Heun ODE (and its solutions) are determined by the so-called Riemann P-symbol and the *accessory* parameter $Q$[44]:

$$P\left\{\begin{matrix} 0 & 1 & a & \infty & \\ 0 & 0 & 0 & \alpha & ; s \\ 1-\delta_1 & 1-\delta_2 & 1-\delta_3 & \beta & \end{matrix}\right\} = P\left\{\begin{matrix} 0 & 1 & -\zeta^2 & \infty & \\ 0 & 0 & 0 & 0 & ; s \\ 2i\frac{w}{3} & 2i\frac{w}{3}\zeta & 2i\frac{w}{3}\zeta^2 & 2 & \end{matrix}\right\} \tag{B6}$$

$$Q = iq^2\zeta/\sqrt{3}\,, \tag{B7}$$

where $\zeta = e^{-i2\pi/3}$ as defined above. The first row of the Riemann P-symbol contains the RSPs and the other 2 rows the corresponding characteristic exponents. Since the $b_i$'s determine the characteristic exponents: $\delta_i = 1 + 2b_i = 1 + 2(\pm iwu_i/3)$, we have the freedom to choose the sign of each $b_i$. We opt for the solutions $b_i = -iwu_i/3$, motivating our choice by the in-falling boundary condition at the horizon used in the main body, which requires $A_y \sim (1-u)^b$ near $u = 1$ with $b = -iw/3$. Thus the choice $b_1 = b$.

We see that the frequency $w$ is the "central" parameter, since it determines 3 of the 4 non-zero characteristic exponents, the exception being the one at $\infty$. The momentum $q$ enters only via the accessory parameter $Q$.

#### *a. Solution*

There are $8 = 2 \times 4$ local solutions to the Heun equation[44,45]: 2 per RSP. The one corresponding to the RSP $s = 0$ and the characteristic exponent 0 is called the *local Heun function* and denoted by $H\ell(a, Q; \alpha, \beta, \delta_1, \delta_2; s)$. It is normalized to 1 at $s = 0$. Incidentally, amongst the 8 local solutions, this is the one that is relevant for us since the $s = 0$ RSP corresponds to the black hole horizon at $u = 1$, and this is precisely where we apply the in-falling boundary condition. Interestingly, it is known that when $\delta_1$ is a non-positive integer, $H\ell$ is ill-defined[44]. Since $\delta_1 = 1 - 2iw/3$, this actually occurs at the special zipping frequencies identified in the bulk, $w_n^{\rm zip} = -i3n/2$, $n \in \mathbb{Z}^+$. As we discuss

below, these correspond to poles of $H\ell$. The solution of Eq. (B1) can thus be expressed using $H\ell$:

$$A_y = (1-\zeta)^{-iw/3} s^{-iw/3} (1-s)^{-iw\zeta/3} (1-s/a)^{-iw\zeta^2/3} \times H\ell\left(-\zeta^2, i\frac{q^2}{\sqrt{3}}; 0, 2, 1-2i\frac{w}{3}, 1-2i\frac{w\zeta}{3}; s\right) \tag{B8}$$

$$s = \frac{u-1}{\zeta-1} \tag{B9}$$

where at the horizon, $s = 0 = u-1$, $F = A_y/(1-u)^{-iw/3}$ is normalized to unity. Note the appearance of the variable $u$ in the normalization condition instead of $s$.

The local Heun function has a Fuchs-Frobenius series expansion in the disk $|s| < 1$, $H\ell(a, Q; \alpha, \beta, \delta_1, \delta_2; s) = \sum_{j=0}^{\infty} c_j s^j$, with the coefficients satisfying[45]

$$c_0 = 1\,, \quad c_1 a\delta_1 - c_0 Q = 0 \tag{B10}$$

$$R_j c_{j+1} - (Q_j + Q)c_j + P_j c_{j-1} = 0 \tag{B11}$$

The parameters $P_j, Q_j, R_j$ used in the recursion relations are defined as

$$P_j = (j-1+\alpha)(j-1+\beta) \tag{B12}$$

$$Q_j = j[(j-1+\delta_1)(1+a) + a\delta_2 + \delta_3] \tag{B13}$$

$$R_j = a(j+1)(j+\delta_1) \tag{B14}$$

Contrary to its simpler hypergeometric cousins, no closed-form solution for the $c_j$ is known in general. Nonetheless, it can be efficiently implemented and we have explicitly verified that the series solution matches the one obtained by numerically solving the initial-value problem.

Using Eq. (20), the solution for the transverse correlator $C_{yy}(w,q) = \Pi^T(w,q)$ can be thus expressed as

$$\frac{\Pi^T(w,q)}{-\chi_0} = iw + \frac{e^{i5\pi/6}}{\sqrt{3}} \frac{\partial_s H\ell(-\zeta^2, i\frac{q^2}{\sqrt{3}}; 0, 2, 1-2i\frac{w}{3}, 1-2i\frac{w\zeta}{3}; s_0)}{H\ell(-\zeta^2, i\frac{q^2}{\sqrt{3}}; 0, 2, 1-2i\frac{w}{3}, 1-2i\frac{w\zeta}{3}; s_0)} \tag{B15}$$

where $s_0 = 1/(1-\zeta) = -e^{i5\pi/6}/\sqrt{3}$ is the value of $s$ at $u = 0$.

In special cases, the Heun function can be simplified. For instance, when $\alpha\beta = Q = 0$, the Heun equation looses its RSP at $s = \infty$ and is said to be trivial. In our case, this happens when the momentum vanishes, $q = 0$. It was previously found[3] that the $q = 0$ EoM for $A_y$ can be analytically solved: $A_y = e^{iwz/3}$, where the so-called tortoise coordinate reads $z(u) = -\ln(1-u) - \zeta\ln(1-u/\zeta) - \zeta^2\ln(1-u/\zeta^2)$ (see Ref. 4 for instance). Equivalently, $A_y = (1-u)^{b_1}(1-u/\zeta)^{b_2}(1-u/\zeta^2)^{b_3}$ and the Heun function $H\ell$ is simply a constant, as can be seen from Eq. (B8), or directly from the recursion relation given above. In that case, using Eq. (B15) we recover $\Pi^T(w,q) = -i\chi_0 w$ since $\partial_s H\ell = 0$. In some other cases, the Heun equation also looses a singularity and can be mapped to the hypergeometric equation[44], for e.g. when $\delta_3 = 0$, $Q = \alpha\beta a$ or when $Q = \delta_1 = 0$. For our ODE, this always implies $q = 0$ and is thus of no interest.

We make a remark regarding the QNMs of $\Pi^T = -\chi_0 A_y'(0)/A_y(0)$. As remarked above, $H\ell$ in Eq. (B15) has poles directly at the zipping frequencies $w_n^{\rm zip} = -i3n/2$, $n \geq 1$. These correspond to poles of $A_y(0)$ but not to zeros of $\Pi^T$ since they are canceled by the poles of $A_y'(0)$, which are given by the poles of the derivative of $H\ell$. Thus, only the zeros of $A_y'(0)$, i.e. those of $H\ell$, give the QNM poles of $\Pi^T$.

### 2. $\gamma \neq 0$: more singular points

We now consider the $A_y$-EoM including the 4-derivative term with coupling $\gamma$:

$$A_y'' + \left(\frac{f'}{f} + \frac{g'}{g}\right) A_y' + \frac{w^2 - q^2 f(1-8\gamma u^3)/g}{f^2} A_y = 0\,, \qquad f(u) = 1 - u^3\,. \tag{B16}$$

The main difference with the $\gamma = 0$ equation is the appearance of the term $g'/g$, where $g = 1 + 4\gamma u^3$. The equation is again Fuchsian, but when $\gamma$ is finite and satisfies $|\gamma| < 1/12$, it has 3 additional RSPs compared with Eq. (B1), for a total of 7 RSPs. The new RSPs are the zeros of $g(u)$:

$$-\frac{\mathrm{sgn}(\gamma)}{(4|\gamma|)^{1/3}}(1, \zeta, \zeta^2) =: (v_1, v_2, v_3) \tag{B17}$$

Thus, they differ from the 3 at $\gamma = 0$ by a factor of $-\mathrm{sgn}(\gamma)/|\gamma|^{1/3}$. The RSP at $\infty$ remains. The 6 finite RSPs, $\{u_i, v_i\}$, are shown in Fig. 15 for both signs of $\gamma$.

The additional 3 RSP found at finite $\gamma$, however, play a different role from the original 3 finite ones, $\{u_i\}_{i=1}^3 = \{1, \zeta, \zeta^2\}$. This is expected on physical grounds: the latter are the horizons of the black hole ($u = 1$ is the real horizon, while the other are the "complex horizons") and as such lead to singularities in the metric. The new ones gained at finite $\gamma$ have nothing to do with the metric (the gauge field is in the probe limit) and they only affect the EoM of the gauge field. This can be seen more mathematically as well: *the characteristic exponents of the $v_i$ RSPs vanish identically.* Moreover, their presence does not affect those of the $u_i$, which were found to be $\pm iwu_i/3$. One of the characteristic exponents of the RSP at $\infty$ changes however from 2 to 5, as must be the case because of Fuch's relation: $\sum_\alpha(\rho_1(\alpha) + \rho_2(\alpha) - 1) = -2$, where $\alpha$ sums over all RSPs and the $\rho_i$ are the 2 exponents associated with each point.

Finally, we note that the EoM for the S-dual gauge field $\hat{A}_y$, Eq. (29), has 3 additional RSPs, for a total of 10 RSPs. The new ones are the zeros of $1 - 8\gamma u^3$: $(\hat{v}_1, \hat{v}_2, \hat{v}_3) = \frac{\mathrm{sgn}(\gamma)}{(8|\gamma|)^{1/3}}(u_1, u_2, u_3)$. Just like the $v_i$, these also have frequency and momentum independent characteristic exponents, in this case $\{0, 1\}$ instead of $\{0, 0\}$ for the $v_i$. From Fuch's relation (mentioned in the previous paragraph), we see that the presence of these RSPs does not alter the characteristic exponents of the RSP at $\infty$, making them even more innocuous than the $v_i$. Indeed, we note that they have the same characteristic exponents as a *regular* point.


[1] S. Sachdev, *Quantum Phase Transitions*, 2nd ed. (Cambridge University Press, England, 2011).
[2] J. M. Maldacena, Adv.Theor.Math.Phys. **2**, 231 (1998), arXiv:hep-th/9711200 [hep-th].
[3] C. P. Herzog, P. Kovtun, S. Sachdev, and D. T. Son, Phys.Rev. **D75**, 085020 (2007), arXiv:hep-th/0701036 [hep-th].
[4] W. Witczak-Krempa and S. Sachdev, Phys.Rev. **B86**, 235115 (2012), arXiv:1210.4166 [cond-mat.str-el].
[5] M. Greiner, O. Mandel, T. Esslinger, T. W. Hansch, and I. Bloch, Nature **415**, 39 (2002).
[6] I. B. Spielman, W. D. Phillips, and J. V. Porto, Physical Review Letters **98**, 080404 (2007), arXiv:cond-mat/0606216.
[7] M. Endres, T. Fukuhara, D. Pekker, M. Cheneau, P. Schau$\beta$, C. Gross, E. Demler, S. Kuhr, and I. Bloch, Nature (London) **487**, 454 (2012), arXiv:1204.5183 [cond-mat.quant-gas].
[8] X. Zhang, C.-L. Hung, S.-K. Tung, and C. Chin, Science **335**, 1070 (2012), http://www.sciencemag.org/content/335/6072/1070.full.pdf.
[9] A. Ritz and J. Ward, Phys.Rev. **D79**, 066003 (2009), arXiv:0811.4195 [hep-th].
[10] R. C. Myers, S. Sachdev, and A. Singh, Phys.Rev. **D83**, 066017 (2011), arXiv:1010.0443 [hep-th].
[11] K. Damle and S. Sachdev, Phys. Rev. B **56**, 8714 (1997), arXiv:cond-mat/9705206.
[12] We thank one referee for making this suggestion.
[13] D. T. Son and A. O. Starinets, JHEP **0209**, 042 (2002), arXiv:hep-th/0205051 [hep-th].
[14] A. Núñez and A. O. Starinets, Phys. Rev. D **67**, 124013 (2003), arXiv:hep-th/0302026.
[15] P. K. Kovtun and A. O. Starinets, Phys.Rev. **D72**, 086009 (2005), arXiv:hep-th/0506184 [hep-th].
[16] S. A. Hartnoll and C. P. Herzog, Phys.Rev. **D76**, 106012 (2007), arXiv:0706.3228 [hep-th].

[17] S. A. Hartnoll, C. P. Herzog, and G. T. Horowitz, Phys.Rev.Lett. **101**, 031601 (2008), arXiv:0803.3295 [hep-th].
[18] F. Denef, S. A. Hartnoll, and S. Sachdev, Phys.Rev. **D80**, 126016 (2009), arXiv:0908.1788 [hep-th].
[19] M. Bhaseen, J. P. Gauntlett, B. Simons, J. Sonner, and T. Wiseman, Phys.Rev.Lett. **110**, 015301 (2013), arXiv:1207.4194 [hep-th].
[20] D. R. Gulotta, C. P. Herzog, and M. Kaminski, JHEP **1101**, 148 (2011), arXiv:1010.4806 [hep-th].
[21] S. Hartnoll, "Quantum Critical Dynamics from Black Holes," in *Understanding Quantum Phase Transitions. Series: Condensed Matter Physics, ISBN: 978-1-4398-0251-9. CRC Press*, edited by L. Carr (2010) pp. 701–723, arXiv:0909.3553 [cond-mat.str-el].
[22] W. Witczak-Krempa, P. Ghaemi, T. Senthil, and Y. B. Kim, Phys. Rev. B **86**, 245102 (2012), arXiv:1206.3309 [cond-mat.str-el].
[23] E. Witten, (2003), arXiv:hep-th/0307041 [hep-th].
[24] P. Kovtun and L. G. Yaffe, Phys.Rev. **D68**, 025007 (2003), arXiv:hep-th/0303010 [hep-th].
[25] P. Kovtun, Journal of Physics A Mathematical General **45**, 3001 (2012), arXiv:1205.5040 [hep-th].
[26] O. Aharony, O. Bergman, D. L. Jafferis, and J. Maldacena, JHEP **0810**, 091 (2008), arXiv:0806.1218 [hep-th].
[27] J. McGreevy, Adv.High Energy Phys. **2010**, 723105 (2010), arXiv:0909.0518 [hep-th].
[28] S.-S. Lee, (2010), arXiv:1009.5127 [hep-th].
[29] S. Sachdev, Annual Review of Condensed Matter Physics **3**, 9 (2012), arXiv:1108.1197 [cond-mat.str-el].
[30] D. Chowdhury, S. Raju, S. Sachdev, A. Singh, and P. Strack, Phys. Rev. B **87**, 085138 (2013), arXiv:1210.5247 [cond-mat.str-el].
[31] V. Cardoso and J. P. Lemos, Class.Quant.Grav. **18**, 5257 (2001), arXiv:gr-qc/0107098 [gr-qc].
[32] A. S. Miranda, J. Morgan, and V. T. Zanchin, JHEP **0811**, 030 (2008), arXiv:0809.0297 [hep-th].
[33] R. A. Davison and A. O. Starinets, Phys.Rev. **D85**, 026004 (2012), arXiv:1109.6343 [hep-th].
[34] R. A. Davison and N. K. Kaplis, JHEP **1112**, 037 (2011), arXiv:1111.0660 [hep-th].
[35] D. K. Brattan and S. A. Gentle, JHEP **1104**, 082 (2011), arXiv:1012.1280 [hep-th].
[36] The diffusion equation is $\partial_t \psi = \nabla_x^2 \psi$.
[37] We note that a time-reversal symmetric term with a lower number of derivatives can appear in the case of non-abelian symmetries, "$F^3$", and it can affect the charge response when a background charge density is present.
[38] P. Kovtun, D. T. Son, and A. O. Starinets, JHEP **0310**, 064 (2003), arXiv:hep-th/0309213 [hep-th].
[39] M. Brigante, H. Liu, R. C. Myers, S. Shenker, and S. Yaida, Phys.Rev. **D77**, 126006 (2008), arXiv:0712.0805 [hep-th].
[40] K. Thorne, D. MacDonald, and R. Price, *Black holes: the membrane paradigm* (Yale University Press, 1986).
[41] In the limit of $u \to 1$, the EoM becomes:

$$\tilde{p}_1 F' + [b(b-1) - b\tilde{p}_1 + \tilde{p}_2]F = 0 \tag{B18}$$

where $\tilde{p}_n = \lim_{u\to 1}(1-u)^n p_n(u)$ is finite for both $n = 1$ and 2; $b = -iw/3$. As we saw, gauge invariance requires $\tilde{p}_2$ to vanish at $w = q = 0$. When combined with $F(1) = 1$, we obtain $F'(1) \sim w$ at small frequencies.
[42] J. Šmakov and E. Sørensen, Physical Review Letters **95**, 180603 (2005), arXiv:cond-mat/0509671.
[43] R. Fazio and D. Zappalà, Phys. Rev. B **53**, R8883 (1996).
[44] R. S. Maier, ArXiv Mathematics e-prints (2002), arXiv:math/0203264.
[45] DLMF, "NIST Digital Library of Mathematical Functions," http://dlmf.nist.gov/, Release 1.0.5 of 2012-10-01, chapter 31.